

On the Evidence for Cosmic Variation of the Fine Structure Constant (I): A Parametric Bayesian Model Selection Analysis of the Quasar Dataset

E. Cameron^{1*} and A. N. Pettitt¹

¹*School of Mathematical Sciences (Statistical Science), Queensland University of Technology (QUT), GPO Box 2434, Brisbane 4001, QLD, Australia*

Submitted to MNRAS: xx July 2013.

ABSTRACT

We review the evidence behind recent claims of spatial variation in the fine structure constant deriving from observations of ionic absorption lines in the light from distant quasars. To this end we expand upon previous non-Bayesian analyses limited by the assumptions of an unbiased and strictly Normal distribution for the “unexplained errors” of the benchmark quasar dataset. Through the technique of reverse logistic regression we estimate and compare marginal likelihoods for three competing hypotheses—(I) the null hypothesis (no cosmic variation), (II) the monopole hypothesis (a constant Earth-to-quasar offset), and (III) the monopole+dipole hypothesis (a cosmic variation manifest to the Earth-bound observer as a North–South divergence)—under a variety of candidate parametric forms for the unexplained error term. Our analysis reveals weak support for a skeptical interpretation in which the apparent dipole effect is driven solely by systematic errors of opposing sign inherent in measurements from the two telescopes employed to obtain these observations. Throughout we seek to exemplify a ‘best practice’ approach to Bayesian model selection with prior-sensitivity analysis; in a companion paper we extend this methodology to a semi-parametric framework using the infinite-dimensional Dirichlet process.

Key words: Cosmology: cosmological parameters – methods: data analysis – methods: statistical.

1 INTRODUCTION

Recent claims by Webb et al. (2011) and King et al. (2012) of a cosmic dipole signal in the fine structure constant deriving from their extensive compilation of Keck and VLT quasar absorption line measurements have been greeted with a healthy mix of excitement and skepticism by cosmologists at large. While undoubtedly controversial with respect to the prevailing picture of a Copernican Universe, homogeneous in its composition and physical laws on the largest scales, the possibility of *some* late-time variation in the “fundamental constants” has been expressly identified within a number of well-studied cosmological theories. The touchstone for skeptical reaction to these claims was in fact the close alignment between the equator of the alleged dipole and the North–South divide between the sightlines of the two telescopes used to collect these data; the skeptical interpretation being that systematic errors of opposing sign are to blame for the apparent signal. Crucially, while the

presence of an unexplained error term in the quasar dataset has been acknowledged by the Webb et al. team, to-date all estimates of statistical significance for the dipole (i.e., those by the Webb et al. team and their colleagues at UNSW; Berengut, Kava and Flambaum 2012) have been computed under the assumption of strictly unbiased, Normal errors. Hence, the motivation for our Bayesian re-analysis of the dataset under a variety of biased and unbiased, Normal and non-Normal error models.

The Bayesian model selection (BSM) framework used herein aims to identify the most plausible model to explain the observed data (with the hope of minimizing the posterior predictive error) from amongst a pre-defined set of hypotheses (Berger and Pericchi 1996; Kadane and Lazar 2004). The quantitative basis for the BSM procedure is, characteristically, a ratio of marginal likelihoods (Jeffreys 1961; Jaynes 2003); the resulting “Bayes factor” operating much like an automatic Ockham’s Razor favouring simplicity over complexity (cf. Jeffreys and Berger 1992). As a well-motivated, “automatic” procedure to distinguish between rival theories, given even limited or heterogeneous data, BSM has become

* E-mail: dr.ewan.cameron@gmail.com

highly popular in cosmological (and astronomical) research with novel applications (Trotta 2007; van Dyk et al. 2009) now abounding in the literature and user-friendly software packages for marginal likelihood estimation (Weinberg 2012; Feroz et al. 2013) readily available. However, with this powerful machinery at hand it can be all too easy to fall into the trap of naively/lazily applying the BSM technique without due regard for its limitations, most notably the sensitivity of Bayes factors to the chosen priors on the internal parameters of each candidate model. Hence, in the present study we give particular attention to demonstrating the key elements of principled BSM with prior-sensitivity analysis (Kass and Raftery 1995; Gelman et al. 2003); in this endeavour we hope to provide a minimal template for future cosmological BSM studies. Though we restrict the present investigation to the usual case of parametric model selection, in a companion work (Paper II) we extend our methodology to a potentially more challenging semi-parametric formulation.

The structure of this paper is as follows. In the remainder of the Introduction we give a detailed, historical overview of the observational evidence for and against a cosmic variation in the fine structure constant. In Section 2 we describe the Webb et al. team’s publically-available “quasar dataset” and give a preliminary investigation into the nature of the unexplained error term. In Section 3 we propose a number of candidate mathematical forms for the latter, explain our choice of prior densities on their governing parameters, and examine the resulting posterior distribution of each. In Section 4 we briefly review the reverse logistic regression procedure for marginal likelihood estimation, before proceeding to report and compare the latter for each hypothesis plus error model pairing (and to conduct our prior-sensitivity analysis) in Section 5. Finally, we summarize our conclusions and discuss the merits of possible follow-up observational strategies for resolving this debate in Section 6.

1.1 The Fine Structure Constant in a Cosmological Context

Introduced in 1916 by Arnold Sommerfeld to abbreviate a recurring, dimensionless factor in his relativistic extension of the Bohr model for the hydrogen atom, the fine structure constant, α , is now recognized as one of the fundamental coupling terms of quantum electrodynamics (QED). In this context α serves to characterize the strength of the electromagnetic interaction and has been humorously dubbed, “the Peter Sellers of QED” (Borie 1986), owing to the many different roles it plays within this theory: setting the scale for all electromagnetic cross-sections, binding energies, and decay rates; and, of course, the scale of fine structure splitting in atomic and ionic spectral lines (cf. Griffiths 2005).

Defined by the ratio of the squared elementary charge, e^2 , to the permittivity of free space, ϵ_0 , the reduced Planck constant, \hbar , and the vacuum speed of light, c ,

$$\alpha = \frac{e^2}{(4\pi\epsilon_0)\hbar c}, \quad (1)$$

the fine structure constant has an on-Earth laboratory value, known to remarkable precision through exacting experimentation on quantum scale systems, of $\alpha^{-1} \approx 137.035999037(91)$ (Bouchendira et al. 2011; Hanneke, Fogwell and Gabrielse 2008). Though nominally designated a

“constant” there are various theoretical foundations to support a time-/space-varying α , if empirical evidence of such can be definitively established; most notably, within electrodynamic scalar field models (Bekenstein 1982; Carroll 1998) and grand unification theories (Marciano 1984; Brax et al. 2003). An historical evolution (with respect to cosmological time) of the fine structure constant driven by a decreasing speed of light could even offer a compelling solution to the infamous “Horizon Problem”¹ of Big Bang cosmology without inflation (Moffat 1993; Barrow 1999; Albrecht and Magueijo 1999).

At present there exist just a handful of different approaches, both terrestrial and astronomical, through which one may search for this experimentalist’s “Holy Grail”. These include: (i) the in-laboratory comparison of optical atomic clocks (Fortier et al. 2007; Rosenband et al. 2008); (ii) the nuclear modelling of samarium isotopes extracted from the Oklo natural fission reactor (Shlyakhter 1976; Damour and Dyson 1996; Gould et al. 2006) or rhenium extracted from Earth-fallen meteorite samples (Olive et al. 2004); (iii) the cosmological modelling of angular fluctuations in the temperature and polarization of the Cosmic Microwave Background (Rocha et al. 2004; Nakashima, Nagata and Yokoyama 2008; Menegoni et al. 2009; Galli et al. 2010; Calabrese et al. 2011); and/or (iv) the identification of telltale frequency shifts in α -sensitive features of astronomical spectra, most notably the fine structure emission lines of ionized carbon observed in radio waves from distant lensed galaxies (Levshakov et al. 2012; Weiss et al. 2012) and the ionic absorption lines of various species observed in the visible/near-visible light from distant quasars (Webb et al. 1999, 2001; Murphy et al. 2001; Murphy, Webb and Flambaum 2003; Webb et al. 2011; King et al. 2012). After a number of initial disagreements between rival teams—see Lamoreaux and Torgerson (2004), for instance—now resolved, only the post-Millennial quasar-based studies at present claim to have recovered any significant evidence for an evolving fine structure constant.

First identified in 1966 (Burbidge, Lynds and Burbidge 1966; Stockton and Lynds 1966) the distinctive absorption lines apparent to Earth-bound observers at UV-to-optical wavelengths in the light from distant quasars arise from the interaction of this light with ions of various species encountered during its passage through intervening gas clouds; these residing in the extensive halos of both bright, star-forming galaxies and dark proto-galaxies. The potential of these absorption lines (especially the singly and triply ionized silicon [SiII and SiIV] doublets) as probes of the fundamental constants at extra-galactic distances, complementary to the already-used emission line technique (Savedoff 1956; Bahcall and Salpeter 1965), was quickly realized by Bahcall, Sargent and Schmidt (1967) and used to constrain the cosmic variation of α to within $\sim 10\%$ of its on-Earth value ($\Delta\alpha/\alpha = 0.98[0.05]$)² in the direction of one particu-

¹ Namely, the remarkable homogeneity of the Universe beyond even the scale of casual connection under the standard model; that is, over physical separations exceeding the maximum distance traversable since the beginning of time at the speed of light.

² Throughout both the astronomical literature and our analysis herein the particular notation, $\Delta\alpha/\alpha$, is used to represent the fractional offset of the fine structure constant in the extra-

lar quasar (3C 191). Improvements in astronomical instrumentation have since allowed far stronger constraints on α variation to be established through this approach. Ivanchik, Potekhin and Varshalovich (1999), for instance, have demonstrated $|\Delta\alpha/\alpha| < 2.3 \times 10^{-4}$ (95% CI) in the early Universe (at ~ 4 Gyr after the Big Bang; ~ 9.4 Gyr ago) through SiIV doublet observations along nine quasar sightlines from a ground-based Russian telescope (the BTA-6 at the Special Astrophysical Observatory).

To search for cosmic α variation below this limit (of roughly one part in ten thousand) with quasar absorption line spectra requires application of the “many multiplet” (MM) technique (Dzuba, Flambaum and Webb 1999) in which the relative frequency shifts of *multiple* ionic species are simultaneously compared; the transitions of those species relatively insensitive to α variation (e.g. singly ionized magnesium [MgII]) effectively serving as calibration benchmarks for the stronger shifters (e.g. singly ionized iron [FeII]). Implementation of the MM technique necessarily involves a multi-parameter fit to constrain not only $\Delta\alpha/\alpha$ but also a suite of nuisance parameters accounting for the physical structure of the intervening gas cloud (i.e., column density, kinetic temperature, and the dominant line broadening mechanism). Pioneering this technique in 1999 the Webb et al. team (Webb et al. 1999) recovered tentative evidence that α may have been lower in the past from a sample of 30 extra-galactic absorbers spanning $0.5 < z_{\text{abs}} < 1.6$ (here z_{abs} denotes the cosmological redshift of the absorber(s) under study) observed with the Keck telescope ($\Delta\alpha/\alpha = -1.1 [0.4] \times 10^{-5}$). This exciting result was quickly heralded as support for a certain class of cosmological model admitting a decelerating speed of light (Barrow and Magueijo 2000; Davies, Davis and Lineweaver 2002), though the claimed theoretical basis for the well-publicized Davies et al. interpretation—derived from a (mistaken) consideration of black hole thermodynamics—was soon disproven (Carlip and Vaidya 2003). More interestingly from a statistical point of view was the Webb et al. team’s concern for a possible underestimation of the true errors in their quoted uncertainties, with a remarkably strong dip in their α estimates over a narrow redshift interval ($0.9 \lesssim z_{\text{abs}} \lesssim 1.1$) suggesting the presence of an unexplained source of observational error.

Further post-Millennial studies by the same team (Webb et al. 2001; Murphy et al. 2001; Murphy, Webb and Flambaum 2003) with the Keck telescope—expanding their original sample to a total of 141 absorbers and their redshift baseline to $0.2 < z_{\text{abs}} < 3.7$ —ultimately strengthened the apparent weight of evidence for a time-varying fine structure constant beyond the “ 4σ level”; given the particular assumptions of the statistical analysis employed. Chief amongst these the absence of any *bias* in the afore-mentioned unexplained error term—its presence still inferred from a marked excess of the sample variance over that expected from known sources of observational noise, seemingly greatest within the high redshift population. At this time Murphy, Webb and Flambaum (2003) proposed a number of potential explanatory factors for an additional error term unique to high red-

shift systems—including the entry of damped Lyman-alpha absorbers (dense clouds of neutral hydrogen featuring complex velocity structures more challenging to model via the MM technique) into the sample at $z_{\text{abs}} \gtrsim 2$ (where the rest-frame ultra-violet of their characteristic spectral lines is redshifted within the optical window accessible to on-Earth observers). An alternative hypothesis, the imprint of a spatial variation in α (as we describe below), was discounted at this stage as only weakly supported by the available data (according to a bootstrap significance test); see Murphy, Webb and Flambaum (2003).

It was thus a great surprise in 2010 when new $\Delta\alpha/\alpha$ estimates for 154 (primarily Southern hemisphere) absorption systems along 60 quasar sightlines (52 new and 8 in common with the original Keck sample) derived by the same team (King et al. 2012; Webb et al. 2011)—but this time using archival spectra from the Very Large Telescope (VLT) in Chile—appeared to indicate the opposite evolutionary trend with redshift. Namely, that the fine structure constant was in fact higher in the past for these absorbers ($\Delta\alpha/\alpha = 0.154 [0.132] \times 10^{-5}$). To resolve this contradiction the team were forced to resurrect the spatial variation hypothesis, proposing a smooth transition in α across the Universe manifest to the on-Earth observer as a (z -invariant) monopole plus a (z -dependent³) dipole field. We illustrate graphically in Figure 1 the nature of the spatial variation in $\Delta\alpha/\alpha$ under the best-fit model of this form (cf. Section 3) from King et al. (2012) on a color-/symbol-coded map of the celestial sphere. Note the scale of the inferred variation, which is at the $\Delta\alpha/\alpha \lesssim 10^{-5}$ level only accessible (as noted earlier) via the MM technique.

In Figure 2 we present a comparable visualization of the “raw” $\Delta\alpha/\alpha$ variation in the Webb et al. team’s quasar dataset from which the apparent dipole effect was inferred. To this end we compute in each bin of right ascension and declination containing at least one quasar sightline (but typically two or more; noting as well that there are on average 2-3 absorbers per sightline) the weighted mean,

$$\overline{\Delta\alpha/\alpha} = \frac{\sum(\Delta\alpha/\alpha_i)/(\sigma_{\text{obs},i}^2 + \sigma_{\text{sys},i}^2)}{\sum 1/(\sigma_{\text{obs},i}^2 + \sigma_{\text{sys},i}^2)}. \quad (2)$$

Here σ_{obs} and σ_{sys} represent the standard deviations of the explained and unexplained error terms, respectively, in the Webb et al. team’s proposed generative model (which we detail in Section 2). Despite the substantial degree of noise evident in these measurements (note the increase in scale

³ King et al. (2012) in fact consider a variety of candidate functional forms for their dipole model, including a (redshift) z -invariant dipole, a z^β -dependent dipole, and an $r(z)$ -dependent dipole (with $r(z)$ the cosmological lookback distance). All exhibit (bootstrap randomization-based) statistical significances of $\sim 4\sigma$ over a monopole-only null. However, we note that: (i) a z -invariant dipole implies a strong breaking of the Copernican principle—namely, that the Earth-bound observer does not occupy a privileged position within the cosmos; and (ii) the z^β - alternative (which encompasses a close approximation to the $r(z)$ -model at $\beta \approx 0.3$) already appears from the King et al. (2012) study to be an over-fitting of the available data. Hence, we focus exclusively on the (monopole+) $r(z)$ -dipole scenario in the present analysis. For reference, this was also the approach taken by Berengut, Kava and Flambaum (2012).

galactic system under study from its on-Earth laboratory value, i.e., $\Delta\alpha/\alpha = [\alpha - \alpha_{\text{Earth}}]/\alpha_{\text{Earth}}$.

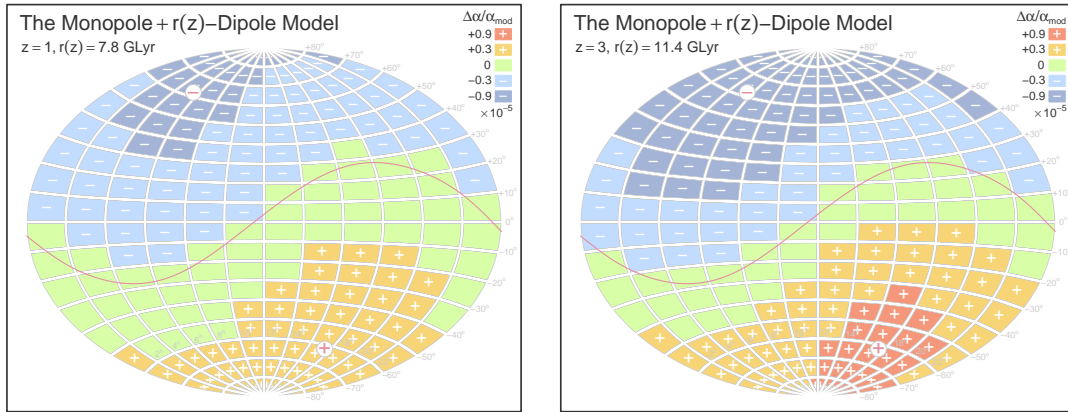


Figure 1. Visualization of the monopole+ $r(z)$ -dipole model (cf. Section 3) for explaining the apparent spatial variation of the fine structure constant proposed by the Webb et al. team. The fractional difference of the fine structure constant from its on-Earth value under this model, $\Delta\alpha/\alpha_{\text{mod}}$, as a function of the observational sightline for the best-fit solution of King et al. (2012) is shown at $z = 1$ in the lefthand panel and that at $z = 3$ in the righthand panel (with the color-/symbol-coding explained in the top-right legend of each). The maximum, minimum, and equator of the key North–South dipole component of this model are overlaid as well for reference.

with respect to that of Figure 1) one may yet discern an excess of negative $\Delta\alpha/\alpha$ estimates in the far North and an excess of positive $\Delta\alpha/\alpha$ estimates in the far South as per the dipole hypothesis. Though, in anticipation of the skeptical interpretation of these results (i.e., that biases of opposite sign in the measurements from each telescope are to blame for the apparent North–South divergence), we note also that the equator of the alleged dipole provides a near perfect subdivision of the sample into its VLT and Keck constituents.

A “ 4σ level” significance for the spatial variation hypothesis was calculated by King et al. (2012) through a bootstrap randomization of $\Delta\alpha/\alpha$ estimates across sightlines and surveys against the simple monopole (i.e., time-/space-invariant with constant [non-zero] Earth-to-quasar offset) alternative—a result echoed by Berengut, Kava and Flambaum (2012) in their review of the dataset using the Akaike Information Criterion, the F statistic, and the “error ellipsoid method”. With the new VLT sample apparently just as subject to unexplained measurement noise as the original Keck dataset, however, a number of strong assumptions were required to justify the significance testing procedures employed. In particular, it was considered necessary to treat the aforesaid as strictly Normal and strictly unbiased (viz. zero mean and mode). Assessing the impact of these assumptions, which are easily relaxed within a Bayesian framework as we demonstrate herein, thus represents an essential “next step” in the analysis of this observational benchmark given the profound implications for both fundamental physics and cosmology if the dipole interpretation is to become accepted.

Following the extensive world-wide media coverage of their work⁴ the Webb et al. team’s spatial variation hypothesis was strongly criticized in a number of public forums, including the popular science blogs, “Uncertain Principles” by Chad Orzel and “Cosmic Variance” by Sean Carroll. The former citing the evident alignment of the alleged dipole’s equator with the coverage overlap of the Keck and VLT

telescopes (cf. Figure 2) as an indicator that biases of opposite sign in the observations from each might well be to blame; and the latter citing the extraordinarily low mass-energy budget ($\sim 10^{-42}$ GeV) for the underlying scalar field implied by the cosmic expanse of the fitted dipole. From a Bayesian perspective these objections may be viewed as disagreements over the relative prior probabilities of competing proposals. Namely, the degree to which the particular model for the unexplained error term adopted by the experimenters should be favoured over some alternative model (or family of models), and the degree to which the null hypothesis (of a time-/space-invariant α) should be favoured “theoretically” over the proposed dipole hypothesis.

2 THE QUASAR DATASET

In this study we examine the publicly-available quasar dataset of Webb et al. (2011): a single catalogue listing for each of the 295 intervening absorbers (141 Keck plus 154 VLT) identified along the 131 quasar sightlines probed to-date their MM-based estimates of z_{abs} , $\Delta\alpha/\alpha$, and σ_{obs} ; the last a standard deviation characterizing the uncertainty in each $\Delta\alpha/\alpha$ estimate arising from explained sources of observational error. Also listed are the J2000 identifier (encoding right ascension and declination in the equatorial coordinate system) and redshift, z_{qua} , of each background quasar, the telescope on which the corresponding observation was made, and the ε_{sys} group to which that observation has been assigned for error analysis—namely, VLT, Keck low contrast (LC), or Keck high contrast (HC). An additional flag highlights two “suspect” absorbers in this catalogue—the $z_{\text{abs}} = 1.542$ system toward J00048–415728 and the $z_{\text{abs}} = 2.84$ system toward J194454+770552. These objects were omitted from the Webb et al. team’s most recent work, and so for consistency are omitted from our reanalysis as well. The quasar dataset thus described is available in electronic form from Professor Michael Murphy’s homepage at the Swinburne University of Technology.

⁴ See, for example, the 23 October 2010 issue of New Scientist magazine (#2783), or the 2 September 2010 issue of The Economist magazine.

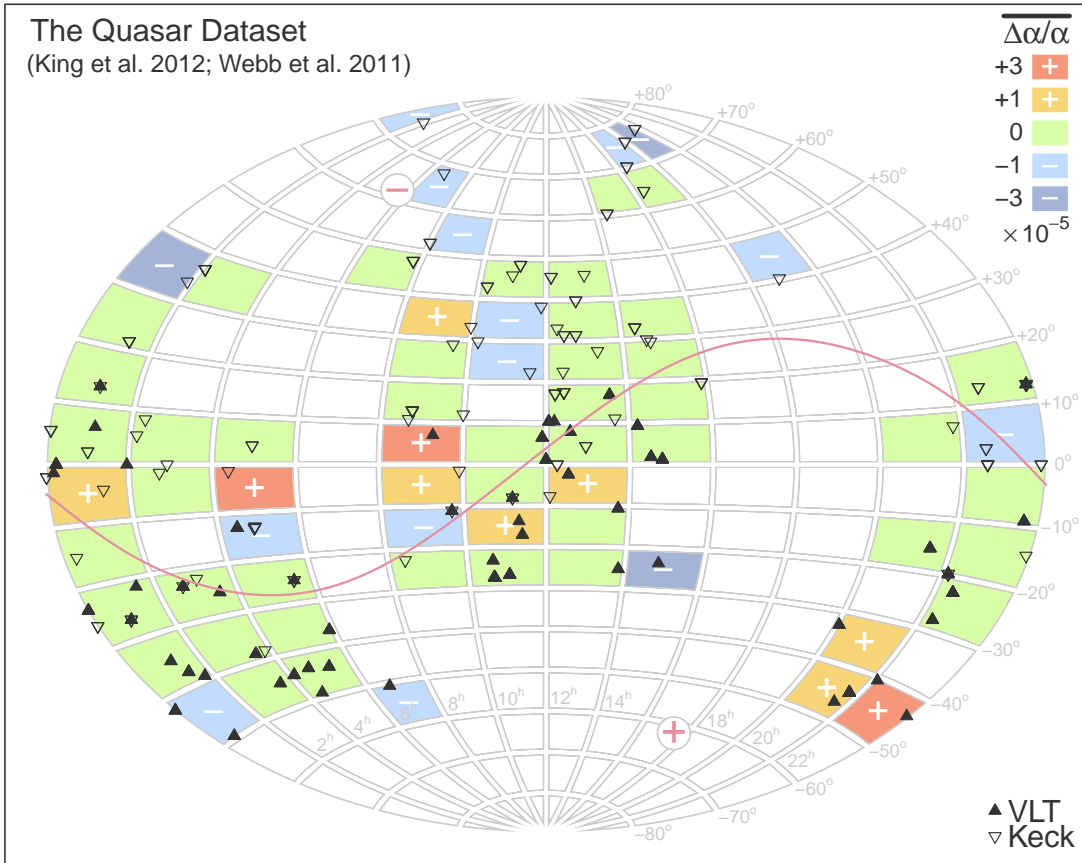


Figure 2. Visualization of the apparent dipole signature in the King et al. (2012) / Webb et al. (2011) quasar dataset. Each quasar sightline in the sample is marked here on a projection of the sky based on the J2000 equatorial coordinate system; with solid-symbols denoting VLT observations and open symbols Keck observations. Note that for most of these quasars there are multiple intervening absorbers providing independent measurements of $\Delta\alpha/\alpha$ along the sightline. The apparent spatial variation of this observable is illustrated via a color-/symbol-coding (detailed in the top-right legend) of its weighted mean in each of the indicated subdivisions. The maximum, minimum, and equator corresponding to the best-fit monopole+ $r(z)$ -dipole solution of the King et al. (2012) paper are overlaid as well for reference.

2.1 Explained Errors

An astronomical spectrograph, such as HIRES on Keck or UVES on the VLT, uses a high-resolution diffraction grating to isolate distinct wavelength components of the incoming light, projecting these onto a charge-coupled device (CCD) for digital intensity measurement. The capture of a raw astronomical spectrum thus constitutes a photon counting experiment in which the count in each pixel of the CCD represents a single draw from a Poisson distribution with mean value set by the integrated flux intensity of light (within a narrow wavelength interval) from the observed source *plus* a contaminating contribution from the background sky and even possibly other non-target emission (e.g. stray light from other bright sources in the field of view); all *modulated* (i.e., non-linearly transformed) by the inherent response characteristic of the telescope and device. In the Webb et al. team’s analysis multiple such raw spectra for each quasar were sourced from the Keck and VLT archives and reduced (i.e., combined and “cleaned”) to single sequences of (high quality) absorption line profiles ready for modelling. The reduction process necessarily involves yet further complex transformations of the raw data

(including “stacking”, “flat fielding”, “bias frame subtraction”, “wavelength calibration”, “cosmic ray removal”, and “continuum subtraction”; the essential cleaning and calibration procedures of precision CCD photometry), which ultimately correlate to some extent both nearby and not-so-nearby pixels in the output profile sequence. However, given the almost overwhelming complexity of accounting directly for each stage of the data reduction pipeline in a statistical modelling context the extent of this correlation is assumed negligible—as is standard practice in the field⁵—with each pixel in the reduced spectrum ultimately treated as independent of all others and assigned an observational standard deviation, σ_i .⁶

⁵ Substantial research efforts are, however, underway to develop Bayesian techniques for modelling more faithfully the complete observational reduction process; see, for example, the recent thesis on this topic by Bosch (2011).

⁶ For further details of this reduction process and the rules applied for “error bar propagation” therein the interested reader may refer, for instance, to the official UVES data reduction cookbook available online.

As noted earlier the MM method for deriving from the reduced spectrum a $\Delta\alpha/\alpha$ estimate for each intervening absorber involves a complex multi-parameter fit across its signature absorption lines. Due to both natural (collisional) and Doppler (thermal and/or turbulent) broadening, the imprint of each line will be typically spread out over multiple resolution elements and a profile function thus required to characterize its shape and recover its centroid (i.e., the precise redshift of that component). The Voigt profile function⁷—with three governing parameters: redshift, column density, and velocity width; the latter being constrained jointly (as the kinetic temperature) across all species detected in the thermal broadening case, but treated as independent in the turbulent case—is well-established as the natural basis for this procedure. However, the number of such bases required to accurately model a particular system, itself a function of the number of distinct “velocity components” present in the intervening cloud, is of course *a priori* unknown.

Thus, the Webb et al. team chose to fit each absorber sequentially, starting with a single Voigt profile function for each line and adding components until a “statistically acceptable” solution was achieved (King et al. 2012); with the benchmark for acceptability characterized by a $1/\sigma_i^2$ -weighted sum of squared residuals (WSSR) approximately equal to the number of pixels fit minus the number of free parameters (dubbed, “the degrees of freedom”, in their analysis though the fitted model is in fact non-linear). The known limitations of the WSSR as a stopping criterion for model selection (cf. Mallows 1995; Andrae, Schulze-Hartung and Melchior 2010) may well contribute to the unexplained errors of the quasar dataset discussed below. Of those Voigt profile models (both thermal and turbulent) tested up to this maximum number of components the model with minimum Akaike Information Criterion (corrected for small n) was then selected as the best choice for *refitting* with $\Delta\alpha/\alpha$ (now) a free parameter. Having located (via a downhill gradient-type search) the WSSR-minimizing (likelihood-maximizing) solution to this final model the Webb et al. team estimate the magnitude of their explained error term, σ_{obs} , from the local curvature of the likelihood surface in $\Delta\alpha/\alpha$; adopting the Normal approximation, $\varepsilon_{\text{obs}} \sim \mathcal{N}(0, \sigma_{\text{obs}}^2)$. The validity of this approximation to the shape of the likelihood surface in the stated context has been confirmed via Markov Chain Monte Carlo (MCMC) exploration, as described by King et al. (2010).

2.2 Unexplained Errors

As mentioned in the Introduction this estimate of the uncertainty in $\Delta\alpha/\alpha$ derived during profile fitting and governed by the (photon counting) realization noise of the observed spectrum has been declared insufficient by the Webb et al. team

to explain the apparent noise level in the quasar dataset. Numerous possible reasons for this have been proposed and discussed at length by Murphy, Webb and Flambaum (2003) and King et al. (2012). These may be divided broadly into two classes: (i) methodological limitations of the fitting procedure rendering inadequate the adopted ε_{obs} distribution, or (ii) hitherto unmodelled sources of additional noise (possibly systematic). From the first class we note the neglected impact of structural uncertainty in the profile fit with regard to the choice of line broadening mechanism and number of velocity components to include; with perhaps a tendency toward underestimation of the latter owing to the known pitfalls of the WSSR stopping criterion adopted. From the second class we have the chance blending of lines from absorbers at different redshifts, and/or run-to-run errors in the wavelength calibration solution (King et al. 2012). Dedicated investigations of the latter by Griest et al. (2010) and Whitmore, Murphy and Griest (2010) have exposed the presence of intra-order velocity shifts against iodine cell reference spectra imaged on both the HIRES and UVES spectrographs of sufficient magnitude to potentially impact on estimates of the fine structure constant; see also the novel asteroid-based calibration study of Molaro et al. (2008).

To account for the inadequacy of ε_{obs} in their analysis the Webb et al. team suppose the existence of a Normally-distributed error term, $\varepsilon_{\text{sys}} \sim \mathcal{N}(0, \sigma_{\text{sys}}^2)$, adding strictly unbiased (zero mean and mode) noise to their $\Delta\alpha/\alpha$ estimates (Webb et al. 2011; King et al. 2012; Berengut, Kava and Flambaum 2012). For each of their monopole and/or dipole hypotheses tested against the quasar dataset the authors constrain the magnitude (viz. standard deviation) of this error term, σ_{sys} , through a Least Trimmed Squares (LTS) procedure (Rousseeuw 1984) in which both its estimate and the best-fitting set of hypothesis parameters (under a WSSR-based likelihood function including this additional error term) are refined in an iterative manner. For the specific monopole+ $r(z)$ -dipole hypothesis examined herein (Equation 3 below) the authors estimate $\sigma_{\text{sys}} \approx 0.858 \times 10^{-5}$ for their VLT sub-sample (or ε_{sys} group), $\sigma_{\text{sys}} \approx 1.630 \times 10^{-5}$ for the sub-sample of their Keck absorbers with high contrast observations (the Keck HC ε_{sys} group), and $\sigma_{\text{sys}} \approx 0$ for the remainder of their Keck absorbers with low contrast observations (the Keck LC ε_{sys} group).

Hence, under the Webb et al. team’s final model for both their explained and unexplained errors the total uncertainty in each $\Delta\alpha/\alpha$ estimate is treated as $\varepsilon_{\text{tot}} \sim \mathcal{N}(0, \sigma_{\text{tot}}^2)$ where $\sigma_{\text{tot}}^2 = \sigma_{\text{obs}}^2 + \sigma_{\text{sys}}^2$ (with σ_{obs} unique to each absorber and σ_{sys} shared across each ε_{sys} group). After outlining for reference the mathematical form of the monopole+ $r(z)$ -dipole hypothesis below we proceed to examine the σ_{obs} - and σ_{tot} -scaled residuals about its best-fit solution from the King et al. (2012) study as a preliminary (and largely qualitative) evaluation of this simple error treatment.

2.3 Mathematical Form of the Dipole

The monopole+ $r(z)$ -dipole hypothesis considered by King et al. (2012) and Berengut, Kava and Flambaum (2012) takes the functional form:

$$\Delta\alpha/\alpha_{\text{mod}|\mathbf{x}_i, \theta_m} = m + B \times r(z_i) \cos(\phi) [\text{ra}_i, \text{dec}_i, \text{ra}_d, \text{dec}_d] \quad (3)$$

⁷ The Voigt profile function (Kendall 1938; Nason 2006) corresponds in shape to the probability density of a continuous random variable defined as the sum of two independent random variables of standard forms—a Normal and a Cauchy. For a more detailed description of the use of the Voigt profile function in the modelling of astronomical spectra the interested reader may refer to (in particular, Appendix A of) Michael Murphy’s PhD thesis also available online.

with $\mathbf{x}_i = \{\text{ra}_i, \text{dec}_i, r(z_i)\}$ the vector of explanatory variables for the i th absorber, $\boldsymbol{\theta}_m = \{m, B, \text{ra}_d, \text{dec}_d\}$ a vector of input model parameters, and $\cos(\phi)[\cdot]$ a function returning the cosine of angular separation between the observational sightline and dipole vector. Given right ascension in hours and declination in degrees the latter may be computed as:

$$\cos(\phi) = \frac{\sin(\text{dec}_i) \sin(\text{dec}_d) + \cos(\text{dec}_i) \cos(\text{dec}_d) \cos(15 \times [\text{ra}_i - \text{ra}_d])}{\cos(\text{dec}_i) \cos(\text{dec}_d)} \quad (4)$$

The lookback distance (cf. Hogg 1999) for each absorber, $r(z_i)$, under the standard cosmological model (here we adopt $\Omega_M = 0.3$, $\Omega_\Lambda = 0.7$, and $H_0 = 70 \text{ km s}^{-1} \text{ Mpc}^{-1}$) is given (in units of GLyr; Giga-Light-years) by:

$$r(z_i) = 13.98 \times \int_0^{z_i} \left[(1+z') \sqrt{0.3 \times (1+z')^3 + 0.7} \right]^{-1} dz'. \quad (5)$$

For reference, we note that the monopole-only null hypothesis corresponds simply to the case of Equation 3 with $B = 0$ —that is, $\Delta\alpha/\alpha_{\text{mod}|\boldsymbol{\theta}_m=\{m\}} = m$ (a non-zero constant); with $\Delta\alpha/\alpha_{\text{mod}|\boldsymbol{\theta}_m=\{m=0\}} = 0$ its strict null counterpart.

2.4 Possible Non-Normality of Residuals

In the top row of Figure 3 we present histograms of the residuals about the best-fit (i.e., $1/\sigma_{\text{tot}}^2$ WSSR-minimizing) solution to the monopole+ $r(z)$ -dipole hypothesis reported by King et al. (2012), scaled by the magnitude of each absorber’s raw observational error term, σ_{obs} , and subdivided by telescope (or, more precisely, ε_{sys} group) and redshift. To limit any sensitivity to the precise functional form for the dipole hypothesis assumed herein we include only those systems lying within $\pm 10^\circ$ of its equator where the contribution of the dipole component is smaller than or equal to the magnitude of the fitted monopole component ($|m| = 0.187 \times 10^{-5}$). If only the explained uncertainties (cf. Section 2.1) represented by $\varepsilon_{\text{obs}} \sim \mathcal{N}(0, \sigma_{\text{obs}}^2)$ were in operation here (and the monopole+ $r(z)$ -dipole hypothesis both true and well fit), then the underlying distributions of these scaled residuals should, of course, themselves be standard Normal. However, this seems unlikely to be the case (as acknowledged by the Webb et al. team’s invocation of the unexplained error term) for either the VLT residuals—which exhibit an unusual bimodality—or the Keck residuals—which exhibit a strong negative skewness. These departures from the standard Normal are further emphasized by the Q-Q plots shown in the top-right inset of each panel.

As described in Section 2.2, under the Webb et al. team’s model for the unexplained uncertainties in the quasar dataset the *total* error on each observation remains zero mean Normal, $\varepsilon_{\text{tot}} \sim \mathcal{N}(0, \sigma_{\text{tot}}^2)$, but takes a broader standard deviation (at least in the case of the VLT and Keck HC ε_{sys} groups) of $\sigma_{\text{tot}} = (\sigma_{\text{obs}}^2 + \sigma_{\text{sys}}^2)^{1/2}$. Rescaling the VLT and Keck HC residuals accordingly we recover those histograms shown in the bottom row of Figure 3. While the scaled residuals now bear a greater similarity to the standard Normal, from a skeptical perspective the rough agreement seen here cannot be considered reassuring, especially given the lack of any strong justification for the supposed form of ε_{tot} . By including below a number of plausible parametric alternatives to the Webb et al. team’s nominal error model

in our reanalysis of the quasar dataset we are able to gauge the influence of the assumed form for the unexplained errors on the apparent dipole significance (cf. Sections 3 to 5).

2.5 Twice-Observed Absorbers

As noted earlier although the Keck and VLT telescopes cover generally well-separated regions of sky—the Hawaii-based Keck being largely restricted to targets in the Northern hemisphere, and the Chile-based VLT restricted to targets in the Southern hemisphere—there nevertheless appears in the Webb et al. dataset an eight quasar intersection of sightlines common to both (evident in Figure 2 as the star-shaped symbols arising from the overlap of the up-triangle and down-triangle symbols used respectively for the VLT and Keck datapoints). Amongst the corresponding population of intervening absorbers thus probed there are eleven twice-observed; that is, detected at matched spectroscopic redshifts in the spectra from both instruments (which feature quite different observational selection functions—owing to the unique resolution and wavelength coverages of each—and hence do not necessarily return *identical* sets of absorbers). The pairwise comparison of Keck and VLT $\Delta\alpha/\alpha$ estimates for these twice-observed systems offers a “first-order” test of the unbiased error hypothesis questioned by Chad Orzel and others skeptical of the Webb et al. team’s conclusions.

The eleven scaled differences, $[\Delta\alpha/\alpha_{\text{Keck}} - \Delta\alpha/\alpha_{\text{VLT}}]/(\sigma_{\text{tot,Keck}}^2 + \sigma_{\text{tot,VLT}}^2)^{1/2}$, so recovered form the ordered list: $\{-1.64, -1.40, -0.97, -0.75, -0.56, -0.52, -0.34, -0.09, 0.17, 0.27, 0.30\}$ (rounded to the 2nd decimal place). The predominance of negative differences observed here (eight of the eleven) hints at the presence of systematic biases in the $\Delta\alpha/\alpha$ values recovered from one or both of these telescopes; and indeed a Wilcoxon signed-rank test (Wilcoxon 1945) allows rejection of the zero mean difference hypothesis at the 5% significance level ($p = 0.017$). Though admittedly not of overwhelming power due to the small sample size available this result nevertheless serves as further motivation (in addition to the alignment of the alleged dipole’s equator along the coverage overlap of the Keck and VLT telescopes) for the biased error models we consider in our Bayesian reanalysis of the quasar dataset below.

3 GENERATIVE MODELS

Having established our motivation for a Bayesian reanalysis of the quasar dataset, and for exploring in this context both unbiased and biased error terms, in the Introduction and Section 2, respectively, we now proceed to outline formally the generative models and priors required for this endeavour.

3.1 Error Models

In the interests of thoroughness we explore four alternative, parametric forms for the total error term operating in each ε_{sys} group; each candidate form allowing a quite different distribution for the unexplained error component. For reference we denote these, **A**, **B**, **C**, and **D**, respectively, and define as follows:

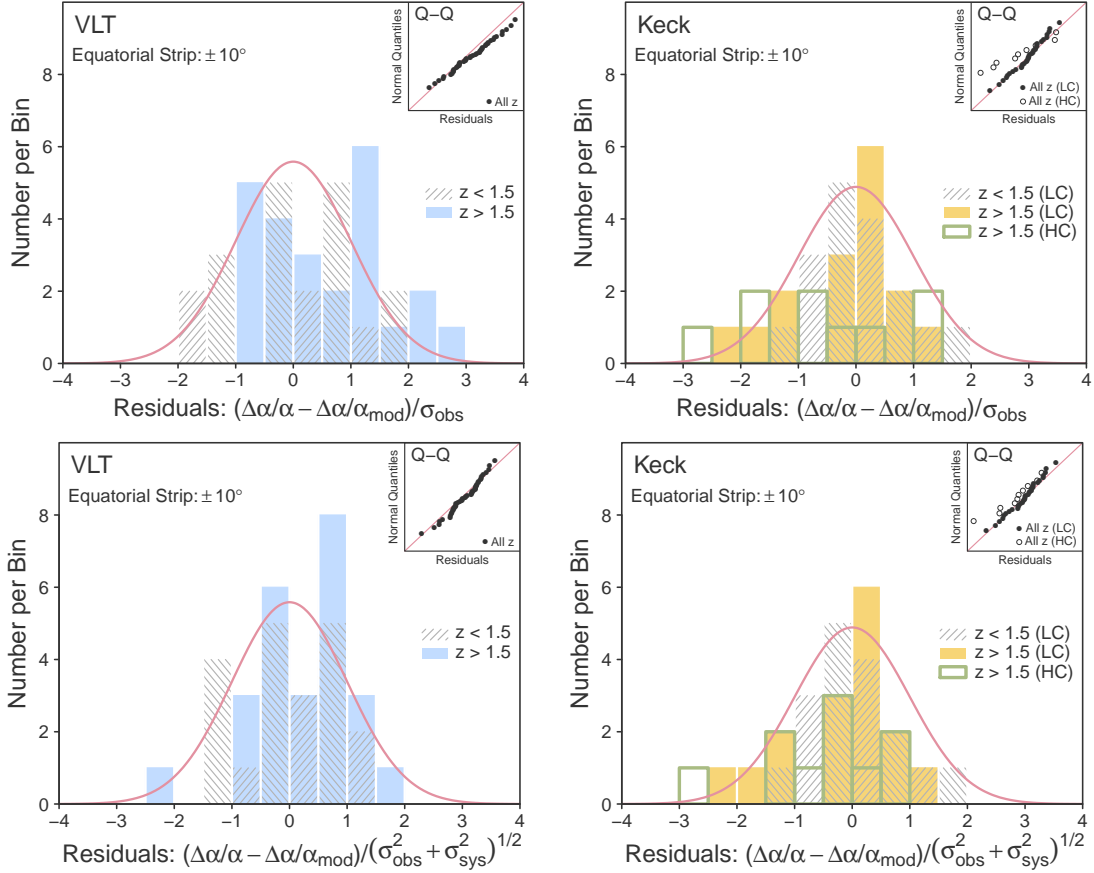


Figure 3. Motivation for our consideration of non-Normal error terms. Each panel contains a histogram of the residuals, $[\Delta\alpha/\alpha - \Delta\alpha/\alpha_{\text{mod}}]$, with respect to the best-fit parameterization of the monopole+ $r(z)$ -dipole hypothesis of King et al. (2012), scaled by the standard deviation of the raw observational error term only in the top row, σ_{obs} , and that of the total error term adopted by Webb et al., $(\sigma_{\text{obs}}^2 + \sigma_{\text{sys}}^2)^{1/2}$, in the bottom row. To limit any sensitivity to the precise functional form adopted for the dipole we include only those systems lying within $\pm 10^\circ$ of its equator (VLT sources on the left; Keck on the right), and we further subdivide each sample by redshift at $z = 1.5$. We draw the reader’s attention to departures in a number of these histograms from the standard Normal form that would be expected if the measurement errors were governed entirely by Normal terms of the magnitude assumed in each row; in particular, the bimodal split about zero in the VLT residuals, and the negative skewness in the Keck residuals. We further emphasise these departures from Normality via the Q-Q (Normal vs. Residual) plots shown as insets in the top-right corner of each panel; the range here (not marked) is exactly -3 to 3 on each axis.

(A) $\varepsilon_{\text{tot}} \sim \mathcal{N}(\beta_{\text{sys}}, \sigma_{\text{obs}}^2 + \sigma_{\text{sys}}^2),$

(B) $\varepsilon_{\text{tot}} \sim \mathcal{V}(\beta_{\text{sys}}, \sigma_{\text{obs}}, \sigma_{\text{sys}}),$ [\mathcal{V} the Voigt distribution]

(C) $\varepsilon_{\text{tot}} \sim \mathcal{N}_{\text{skew}}(\xi_{\text{sys}}, \frac{v_{\text{sys}} w_{\text{sys}}}{\sqrt{\sigma_{\text{obs}}^2 + w_{\text{sys}}^2}}, \sigma_{\text{obs}}^2 + w_{\text{sys}}^2),$

(D) $\varepsilon_{\text{tot}} \sim \begin{cases} \mathcal{N}(-\gamma_{\text{sys}}\sigma_{\text{obs}}, \sigma_{\text{obs}}^2) & \text{with probability } \eta_{\text{sys}}, \\ \mathcal{N}(\gamma_{\text{sys}}\sigma_{\text{obs}}, \sigma_{\text{obs}}^2) & \text{otherwise.} \end{cases}$

Error form **A** corresponds, of course, to the scenario of a Normally-distributed source of systematic measurement noise, $\varepsilon_{\text{sys}} \sim \mathcal{N}(\beta_{\text{sys}}, \sigma_{\text{sys}}^2)$, operating in addition to, and independently of, the explained error, $\varepsilon_{\text{obs}} \sim \mathcal{N}(0, \sigma_{\text{obs}}^2)$. At $\beta_{\text{sys}} = 0$ this equates to the strictly unbiased (i.e., zero mean and mode) error term adopted by King et al. (2012); and we therefore consider this limiting case the *nominal* error model (**A**₀) for our analysis, treating the more general $\beta_{\text{sys}} \neq 0$ case as the default *skeptical* model.

Error form **B**, on the other hand, corresponds to the (undesirable) scenario of a *heavy-tailed* source of Cauchy-distributed measurement noise with location, β_{sys} , and

scale, σ_{sys} , i.e., $\varepsilon_{\text{sys}} \sim \mathcal{C}(\beta_{\text{sys}}, \sigma_{\text{sys}})$ where $f_{\mathcal{C}}(x) = 1/\pi \times \sigma_{\text{sys}}/(\sigma_{\text{sys}}^2 + (x - \beta_{\text{sys}})^2)$, operating in addition to, and independently of, the explained error. As noted in our earlier discussion of absorption line modelling (Section 2.1), the Voigt profile function (cf. Kendall 1938; Nason 2006), \mathcal{V} , provides an analytical expression for the density of such a distribution arising from the convolution of a Cauchy and a Normal. Namely,

$$f_{\mathcal{V}}(x) = \frac{\text{Re}[\omega(z)]}{\sigma_{\text{obs}}\sqrt{2\pi}}, \quad z = \frac{(x - \beta_{\text{sys}}) + i\sigma_{\text{sys}}}{\sigma_{\text{obs}}\sqrt{2}}, \quad -\infty < x < \infty,$$

where $\omega(\cdot)$ in the above denotes the complex error (or “Faddeeva”) function. By allowing, through error form **B**, for the possibility of heavy-tailed behaviour in the unexplained error term we help to ensure the robustness of our conclusions under the Normal error form (**A**) against the possible presence of extreme outliers in the quasar dataset. Though the mean remains undefined for the Cauchy, and thus the Voigt as well, we note that $\beta_{\text{sys}} = 0$ nevertheless gives a zero mode case (**B**₀), which we refer to as “unbiased” for

our purposes and which we examine separately to the more general (skeptical) $\beta_{\text{sys}} \neq 0$ case.

Error form **C** supposes instead a source of *skew Normal* noise, $\varepsilon_{\text{sys}} \sim \mathcal{N}_{\text{skew}}(\varepsilon_{\text{sys}}, v_{\text{sys}}, w_{\text{sys}}^2)$, operating in addition to, and independently of, the explained error. A tendency toward bias in the wavelength calibration solution for a given ε_{sys} group may be one explanation for such an asymmetric distribution in the uncertainties of the quasar dataset. We note here for reference the definition of the skew Normal with normalized shape parameter, v , scale, w , and location parameter, ξ , in terms of the standard Normal density, $\phi(\cdot)$, and distribution function, $\Phi(\cdot)$:

$$f_{\mathcal{N}_{\text{skew}}}(x) = \frac{2}{w} \phi\left(\frac{x - \xi}{w}\right) \Phi\left(\frac{v(x - \xi)}{w\sqrt{1 - v^2}}\right), \quad -\infty < x < \infty,$$

with $-1 < v < 1$ and $w > 0$. We note also that the sum of a (zero mean) Normal, $\mathcal{N}(0, \sigma_{\text{sys}}^2)$, and a skew Normal, $\mathcal{N}_{\text{skew}}(\xi_{\text{sys}}, v_{\text{sys}}, w_{\text{sys}}^2)$, is again skew Normal, with parameters as specified in our definition of error form **C** above. This may be verified, of course, by reference to the characteristic function of the skew Normal distribution; according to Pewsey (2000), $\Psi_{\mathcal{N}_{\text{skew}}(\xi, v, w^2)}(t) = \exp(i\xi t - w^2 t^2/2) \{1 + i\tau(vwt)\}$ where $\tau(x) = \int_0^x \sqrt{2/\pi} \exp(u^2/2) du$ for $x > 0$ and $\tau(-x) = -\tau(x)$. We consider once again a so-called “unbiased” (here zero mode, but *not* mean) case (**C**₀), constructed by solving numerically for ξ_{mode} for each σ_{obs} and $\{v_{\text{sys}}, w_{\text{sys}}\}$ parameter pairing, in addition to the skeptical case of free ξ_{sys} .

Finally, error form **D** corresponds to a scenario of systematic mis-estimation in which $\Delta\alpha/\alpha$ is alternately *under-shot* or *over-shot* by $\gamma_{\text{sys}} \times \sigma_{\text{obs}}$, with probability η_{sys} of the former (and $1 - \eta_{\text{sys}}$ of the latter). Such a bimodal error distribution might well arise as the result of routine mis-identification of the dominant line broadening mechanism (turbulent or thermal) or the number of velocity components present when modelling the observed absorption profile (cf. Section 2.1); and was suggested by the distribution of residuals around the equator of the proposed dipole for the VLT sample (examined in Section 2.4). In the interests of thoroughness, though perhaps not terminological consistency, we also consider an “unbiased” (here zero mean, but not mode) case of this error form (**D**₀) with fixed $\eta = 0.5$.

In Figure 4 we illustrate the nature and diversity of all four candidate forms (**A**, **B**, **C**, and **D**) for the total error term, ε_{tot} , under a variety of arbitrary choices for their governing parameters. As in earlier studies by the Webb et al. team, each of the three ε_{sys} groups of the quasar dataset—namely, the VLT sample, the low contrast (LC) Keck sample, and the high contrast (HC) Keck sample—is treated separately here for error analysis and assigned one of the above. Throughout we employ the notation, **AAA**, **B₀B₀B₀**, **CAD** and so on, to indicate which error form has been assigned to each—Keck LC, Keck HC, and VLT, in that order. We refer specifically to the combination, **AAA**, as our default skeptical model and to the combination, **A₀A₀A₀**, as the nominal error model. With each candidate form admitting two or three governing parameters we must therefore specify a prior density on up a total of nine parameters for a complete error model.

3.2 Error Model Priors

It is widely acknowledged (at least in the statistical literature) that the posterior Bayes factor for Bayesian model selection (BSM) can be remarkably sensitive to the chosen priors on the internal parameters of the various models under consideration (cf. Kass and Raftery 1995). In particular, unlike in the case of general Bayesian inference the interpretation of improper priors is inevitably ill-defined in the model selection context, and the influence of the prior choice cannot simply be assumed to grow negligible with the data volume, n , any faster than an $\mathcal{O}(n^{-1})$ rate. Hence, both the justification of one’s prior selections and a subsequent analysis of the problem-specific prior-sensitivity are essential ingredients of rigorous BSM; the former we present directly below and the latter in Section 5.

In constructing priors on the governing parameters of our error models we are guided by the general observation that the standard deviation of the unexplained error term must be of roughly the same order as the explained error term in this dataset ($\overline{\sigma_{\text{obs}}} \approx 2 \times 10^{-5}$); if it were very much smaller it would presumably have gone unnoticed, while if it were very much larger the Webb et al. team would have been unlikely to have proceeded to hypothesis testing without a better understanding of its origin. Equivalently, its bias (under the skeptical interpretation) should be of comparable magnitude (in $\Delta\alpha/\alpha$) to that of the alleged dipole. Choosing independent Normal densities to describe our prior beliefs regarding the β_{sys} and σ_{sys} of our default skeptical error form (**A**) we reduce the problem of prior specification to one of hyperparameter choice (Chipman, George and McCulloch 2001); and in light of the above we nominate simply, $\pi(\beta_{\text{sys}}) \sim \mathcal{N}(0, \sigma_q^2)$ with (hyperparameter) $\sigma_q = 0.5 \times 10^{-5}$ and $\pi(\sigma_{\text{sys}}) \sim \mathcal{N}_{\text{half}}(0, \sigma_p^2)$ with (hyperparameter) $\sigma_p = 2 \times 10^{-5}$. (Here $\mathcal{N}_{\text{half}}$ denotes the half-Normal distribution, chosen so as to keep the standard deviation parameter, σ_{sys} , strictly positive.)

To promote fairness in the marginal likelihood-based comparison of each model–hypothesis pairing we have attempted to make our priors on the parameters of the remaining three error forms as similar as possible to those of form **A**. Thus, for error form **B** we suppose $\pi(\beta_{\text{sys}}) \sim \mathcal{N}(0, [0.5 \times 10^{-5}]^2)$ for the mode of the underlying Cauchy, but allow a (slightly) larger range of $\pi(\sigma_{\text{sys}}) \sim \mathcal{N}_{\text{half}}(0, [\sqrt{2} \log(2) \times 2 \times 10^{-5}]^2)$ on its scale parameter to match our effective prior on the full width at half maximum (FWHM) of this error form to that of **A** (the standard deviation being undefined for the Cauchy, and thus not available for comparison). For error form **C** we begin by setting our prior on the *unnormalized* skew parameter, $v_{\text{sys}}/\sqrt{1 - v_{\text{sys}}^2}$, of this distribution to a generous, $\mathcal{N}(0, [10]^2)$; which transforms to the following density on the *normalized* skew parameter, v_{sys} , with $a = 10$:

$$f_{\pi(v_{\text{sys}})}(x) = \frac{1}{\sqrt{2\pi a^2}} \exp\left[\frac{-x^2}{2a^2(1 - x^2)}\right] \frac{1}{(1 - x^2)^{3/2}},$$

for $-1 < x < 1$ (zero otherwise). We then match our prior on the standard deviation of the unexplained error term in **C** to that of **A** by setting $\pi(w_{\text{sys}}|v_{\text{sys}}) \sim \mathcal{N}_{\text{half}}(0, [(1 - \frac{2}{\pi} v_{\text{sys}}^2)^{-1/2} \times 2 \times 10^{-5}]^2)$; and likewise to match our priors on the corresponding means we choose, $\pi(\xi_{\text{sys}}|v_{\text{sys}}, w_{\text{sys}}) \sim \mathcal{N}(-v_{\text{sys}} w_{\text{sys}} \sqrt{\frac{2}{\pi}}, [0.5 \times 10^{-5}]^2)$. Finally,

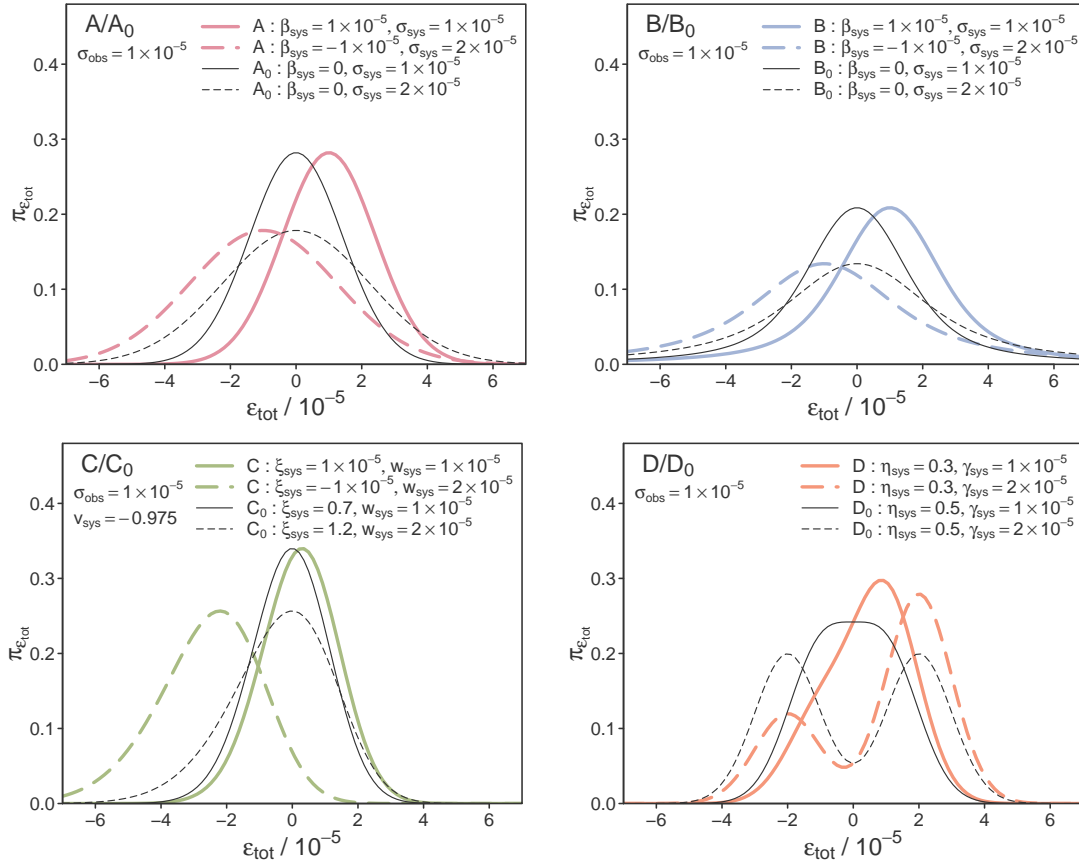


Figure 4. Illustration of the four candidate forms (**A**, **B**, **C**, and **D**) proposed here for modelling the total error term, ε_{tot} , of the quasar dataset. We specify an arbitrary standard deviation of $\sigma_{\text{obs}} = 1 \times 10^{-5}$ for the explained uncertainty component, $\varepsilon_{\text{obs}} \sim \mathcal{N}(0, \sigma_{\text{obs}}^2)$, in these plots, and we indicate the diversity of densities thereby admitted under each corresponding total error term by tracing the output for a variety of selected inputs to its governing parameters (detailed in the top-right legend of each panel). For clarity, the “unbiased” cases of the forms shown here (**A**₀, **B**₀, **C**₀, and **D**₀) are clearly distinguished (via a reduced line thickness) from their general (skeptical) counterparts.

for error form **D**, for which no precise matching of this nature is possible, we simply adopt $\pi(\gamma_{\text{sys}}) \sim \mathcal{N}(0, [0.5 \times 10^{-5}]^2)$ and $\pi(\eta_{\text{sys}}) \sim \text{Beta}_{\text{half}}(15, 15)$ (i.e., “folded” about 0.5 [$f_{0 < x < 0.5}^*$ or $f_{0.5 < x < 1}^* = 2f_{0 < x < 1}$]), favouring a near-symmetric ε_{sys} over a markedly asymmetric one. For the typical absorber with explained error, $\sigma_{\text{obs}} \approx 2 \times 10^{-5}$, this gives a prior expectation on the bias of the unexplained error term in each ε_{sys} group comparable to that of our form **A** benchmark.

Important to note is that we have avoided Uniform priors at the above specification stage; the reasons behind this are two-fold: (i) although computationally convenient, the implication of a Uniform prior choice—that one believes all parameter values within a precise parameter range equally plausible but anything outside this range entirely implausible—is clearly not justifiable for any of these parameters; and (ii) provided the range hyperparameters of a Uniform prior are made sufficiently wide as to encompass the bulk of posterior mass, then their further manipulation has negligible impact on the posterior fit but a profound impact on the corresponding Bayes factor, meaning that such priors can all too easily be manipulated by the unscrupulous practitioner to artificially favour or disfavour some particular model.

3.3 Hypothesis Priors

We apply similar principles with regard to constructing priors on the input parameters, $\theta = \{m, B, ra_d, dec_d\}$, of the Webb et al. team’s proposed monopole+ $r(z_i)$ -dipole hypothesis for the apparent cosmic variation of $\Delta\alpha/\alpha$ (see Equation 3 in Section 2.3). For the strength of the monopole term, m , we adopt a zero mean Normal prior with standard deviation, 0.5×10^{-5} , and for the strength of the dipole term, B , an exponential prior with rate, $1/[0.5 \times 10^{-5}]$. That is, $\pi(m) \sim \mathcal{N}(0, [0.5 \times 10^{-5}]^2)$ and $\pi(B) \sim \text{Exp}(1/[0.5 \times 10^{-5}])$. Supposing *a priori* that the dipole vector might point anywhere on the celestial sphere with equal probability we assign the appropriate uniform priors to both ra_d and the sine of dec_d . Thus, $\pi(ra_d) \sim \text{U}(0, 24)$ and $\pi(\sin(dec_d)) \sim \text{U}(-1, 1)$, i.e., $\pi(dec_d) \sim \cos(dec_d)/2$.

For consistency with the above we also suppose $\pi(m) \sim \mathcal{N}(0, [0.5 \times 10^{-5}]^2)$ for the strength of the monopole in the monopole-only version of the null hypothesis; recall though, our strict null hypothesis is that $\Delta\alpha/\alpha$ remains everywhere zero.

3.4 Likelihood Function

With any stochastic variation in the $\Delta\alpha/\alpha$ estimates of the quasar dataset assumed to arise solely from the combination, ε_{tot} , of the explained and unexplained error terms described by the error models of Section 3.1—and with the realization of this measurement error for any given absorber assumed independent of all others—the likelihood function for the observed data, $\mathbf{y} = \{\Delta\alpha/\alpha_i : i = 1, \dots, 293\}$ with covariates represented as $\mathbf{x}_i = \{\text{ra}_i, \text{dec}_i, r(z_i)\}$, corresponding to a given $\Delta\alpha/\alpha_{\text{mod}}$ and ε_{tot} pairing, M , may be written as:

$$L(\mathbf{y}|\boldsymbol{\theta} = \{\boldsymbol{\theta}_m, \boldsymbol{\theta}_e\}, M, \mathbf{x}_i) = \prod_{i=1}^{293} f_{\varepsilon_{\text{tot}}|\boldsymbol{\theta}_e}(\Delta\alpha/\alpha_i - \Delta\alpha/\alpha_{\text{mod}(M)}|\mathbf{x}_i, \boldsymbol{\theta}_m). \quad (6)$$

Here $\boldsymbol{\theta}_m = \{m, B, \text{ra}_d, \text{dec}_d\}$ (dipole) [or $\{m\}$ (monopole null), or $\{m = 0\}$ (strict null)] denotes the set of input hypothesis parameters, $f_{\varepsilon_{\text{tot}}|\boldsymbol{\theta}_e}$ the ε_{tot} probability density for the particular ε_{sys} group to which the i th absorber belongs, and $\boldsymbol{\theta}_e$ the vector of between six and nine parameters required for a complete error model.

3.5 Posteriors

For each combination of error model and hypothesis tested here (see Section 5 below for a complete enumeration) we have constructed a Markov Chain Monte Carlo (MCMC) sample of 10,000 draws from the posterior ($\beta = 1$), plus a further 10,000 draws from the prior ($\beta = 0$) and each of eight tempered, bridging densities ($\pi(\theta)L(\theta)^\beta$ with β logarithmically spaced between 10^{-5} and 0.5), via the method of “parallel tempering” (also known as MC³; Swendsen and Wang 1986; Geyer 1992). By allowing probabilistic swaps between chains at different temperatures the parallel tempering method can greatly improve mixing relative to the rate of each run separately, particularly for multimodal posteriors. For our within-chain moves we use a symmetric, random walk type proposal; the diagonal variance matrix of which was initialized to our prior variance on each parameter and progressively rescaled toward a target acceptance rate of 0.4 during a 5,000 draw burn-in phase. Although the marginal likelihoods of each model–hypothesis pairing (which we ultimately derive from these chains using the RLR technique described in Section 4 below) are in fact the sole quantities of interest for our Bayesian assessment of the claimed spatial variation in the quasar dataset we nevertheless review briefly here the nature of our posterior inferences for key error model and hypothesis parameters as an aid to understanding the ensuing results.

In Figures 5 and 6 we illustrate the marginal posterior probability densities of those parameters (or combinations thereof) governing the width (viz. standard deviation, or half width half maximum as appropriate in the case of model **B**) resulting from each error form (**A/A**₀ to **D/D**₀, as described in Section 3.1) applied homogeneously across all ε_{sys} groups under both the strict null and dipole hypotheses. (Our posteriors under the monopole-only null hypothesis, and for the two non-homogeneous error model combinations we test, **CAA** and **CAD** [cf. Section 5 below], being roughly intermediate to these representative examples.) Although the inferred width of the unexplained error term for each ε_{sys} group varies somewhat depending upon the error model adopted, the relative ordering of the aforesaid—Keck

LC, VLT, Keck HC (from smallest to largest)—does not. For the “unbiased” case of each model in particular (Figure 6: **A**_{0**A**_{0**A**₀ to **D**_{0**D**_{0**D**₀) we note that the error widths recovered under the null hypothesis are generally somewhat greater than those recovered under the (more flexible) dipole hypothesis—that is, the proposed error forms must necessarily “stretch” to encompass the broader spread of residuals in the former. Interestingly, the Bayesian analysis we present here for the nominal error model (**A**_{0**A**_{0**A**₀) favours a non-zero σ_{sys} of roughly 0.6×10^{-5} (posterior mean) for the Keck LC ε_{sys} group under the strict null hypothesis, in contrast to the $\sigma_{\text{sys}} \approx 0$ Least Trimmed Squares (LTS) estimate reported by King et al. (2012) in their Table 2. This discrepancy presumably arises from the deliberate focus on interquartile width at the expense of (or, purportedly in robustness against) any marked outliers in the latter approach. Our estimates for the other ε_{sys} groups under both the null and dipole hypotheses are nevertheless in fair agreement with their LTS counterparts.}}}}}}

In Figure 7 we present the marginal posterior probability densities of the parameters (or combinations thereof) governing the “bias” (viz. offset of the mode, or in case **D** the mean, from zero) in each of our general (skeptical) error models (applied homogeneously across all ε_{sys} groups) under both the strict null and dipole hypotheses. The degree of bias favoured by these posteriors for each ε_{sys} group varies little between error models but greatly between hypotheses—as expected, larger biases are generally preferred under the strict null hypothesis than under the dipole hypothesis, owing to the inherent (though of course only partial) degeneracy between the North–South dipole and opposing bias scenarios.

Finally, for reference we plot in Figure 8 the joint posterior densities of the key parameter pairings under the monopole+ $r(z)$ -dipole hypothesis—viz. monopole strength–dipole strength (m – B) and right ascension–declination of the dipole vector (ra_d – dec_d)—for error models **AAA**, **A**_{0**A**_{0**A**₀, **CCC**, and **C**_{0**C**_{0**C**₀. While the posteriors corresponding to each error model in the “unbiased” case are both highly concentrated around the maximum likelihood solutions identified by the Webb et al. team under their fitting of the nominal error model (**A**_{0**A**_{0**A**₀)—namely, $\{\text{ra}_d \approx 17.5 \text{ hours}, \text{dec}_d \approx -60 \text{ degrees}\}$ and $\{m \approx -0.2 \times 10^{-5}, B \approx 10^{-6}\}$ —in the biased (skeptical) case the corresponding posteriors are evidently more diffuse and favour markedly a smaller dipole strength.}}}}}}

To discriminate between this plethora of plausible generative models with quasi-degenerate parameters—and to thereby identify the strongest candidate(s) for explaining the apparent spatial variation of the quasar dataset—we now proceed to the Bayesian comparison of marginal likelihoods (cf. Kass and Raftery 1995).

4 REVERSE LOGISTIC REGRESSION

For each hypothesis–error model pairing we estimate the marginal likelihood based on our parallel tempered MCMC draws using the technique of reverse logistic regression (RLR) introduced by Geyer (1994). A common misconception in astronomical studies is that despite having performed extensive parallel tempering to simulate from

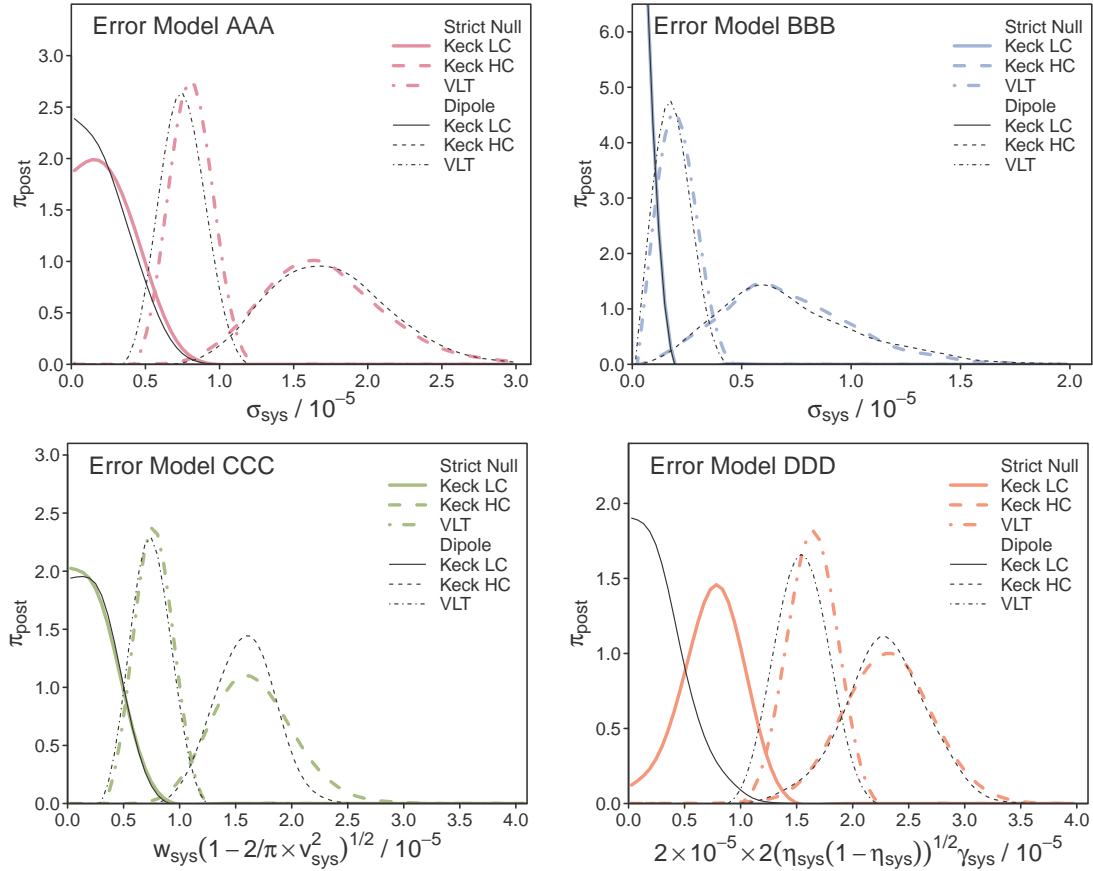


Figure 5. Posterior probability densities for the key parameters (or combinations thereof) governing the underlying error distribution width (viz. standard deviation, or half width half maximum as appropriate in the **BBB** case) of the ε_{sys} component in each of our general (skeptical) error models: **AAA** to **DDD** (homogeneous). In the interests of illustrative clarity only those posteriors corresponding to the strict null (i.e., $\Delta\alpha/\alpha$ everywhere zero) and dipole hypotheses are compared here (our results for the monopole-only null hypothesis being roughly intermediate to these two). Interestingly, although the inferred width of the unexplained error term for each ε_{sys} group varies somewhat depending upon the error model adopted, the relative ordering of the aforesaid—Keck LC, VLT, Keck HC (from smallest to largest)—does not.

the Bayesian posterior it remains necessary to apply a further sampling technique for model selection purposes. In fact, RLR (or the equivalent Density of States summation; Cameron and Pettitt 2013) offers a reliable solution for this scenario, requiring at minimum a set of likelihoods drawn from the prior⁸ and from one other temperature configuration, $\pi(\theta)L(\theta)^\beta$, perhaps the posterior itself ($\beta = 1$). As in our recent update to the **MultiNest** code (INS; Feroz et al. 2013) the RLR algorithm uses a ‘losing the labels’ strategy in which the likelihoods from all specified proposals are pooled together and a recursive computation used to estimate normalizations simultaneously for all except the prior (or other reference density) for which $Z_{\beta(1)=0} = 1$ is assumed known. Though we give below only the RLR formula for the case of parallel tempering between the prior and posterior, the interested reader may refer to our recent review paper (Cameron and Pettitt 2013) for the general formula and its derivation, as well as a variety of novel implementation suggestions.

⁸ Or some suitable alternative reference density; i.e., with known normalization and overlapping support.

Supposing one has drawn a series of $\theta_i^{(j)} \sim \pi(\theta)L(\theta)^{\beta(j)}$ for $i = 1, \dots, n(j)$ and $j = 1, \dots, m$ with $\beta(1) = 0$ and $\beta(m) = 1$, the RLR estimator for the marginal likelihood of the posterior, $\hat{Z} (= \hat{Z}_m)$, and intermediate (bridging) densities, \hat{Z}_j ($1 < j < m$), may be recovered via recursion over the following update equation:

$$\hat{Z}_j = \sum_{j=1}^m \sum_{i=1}^{n(j)} \left(L(\theta_i^{(j)})^{\beta(j)} / \left[\sum_{s=1}^m n(s) L(\theta_i^{(j)})^{\beta(s)} / \hat{Z}_s \right] \right) \quad (7)$$

$$= \sum_{i=1}^n \left(L(\theta_i)^{\beta(j)} / \left[\sum_{s=1}^m n(s) L(\theta_i)^{\beta(s)} / \hat{Z}_s \right] \right). \quad (8)$$

The second line of this equation corresponds to the observation that recovery of the marginal likelihood by this method does not in fact require knowledge of which temperature a particular sample point has been sampled from; only the sampling design itself (the set of $\beta(j)$ and their corresponding $n(j)$) need be known. This is consistent with the description of RLR as a ‘losing the labels’ type scheme (see Kong et al. 2003 for a detailed discussion). For uncertainty estimation Geyer (1994) gives one expression for the asymptotic

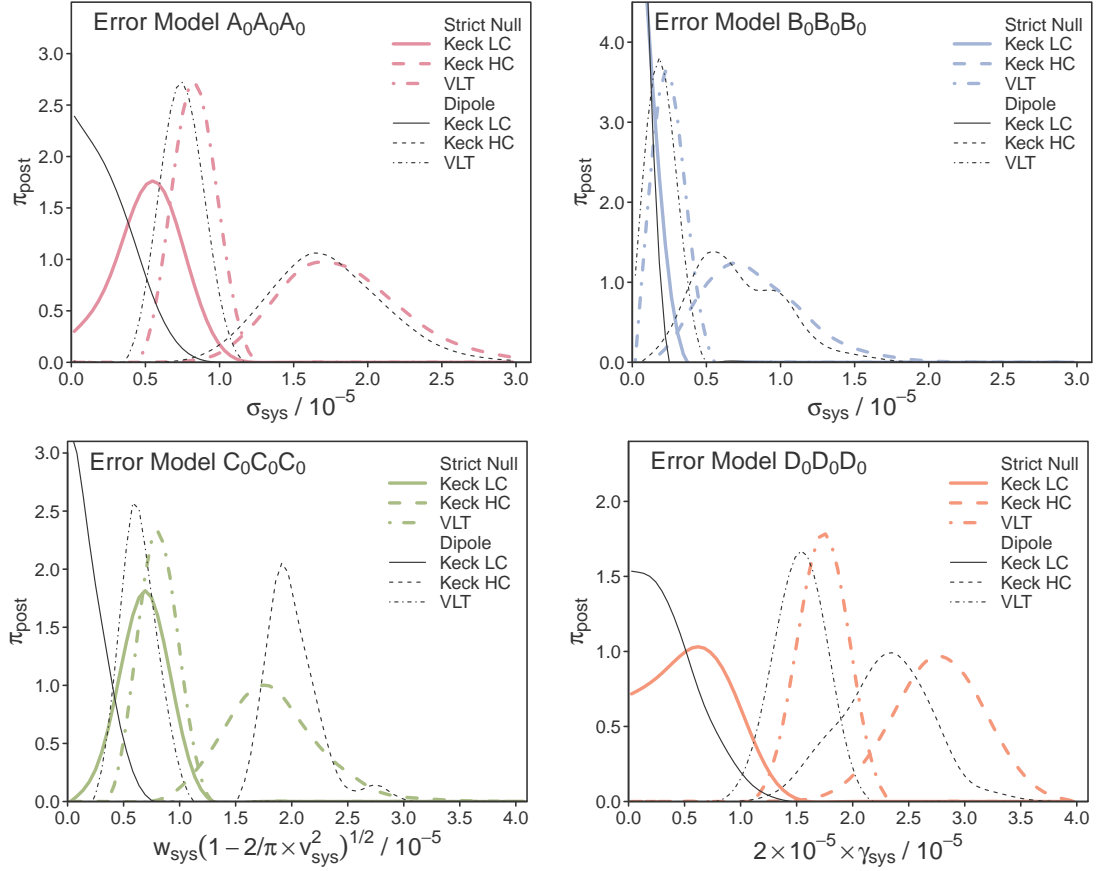


Figure 6. Posterior probability densities for the key parameters (or combinations thereof) governing the underlying error distribution width (viz. standard deviation, or half width half maximum as appropriate in the $B_0B_0B_0$ case) of the ε_{sys} component in each of our “unbiased” error models: $A_0A_0A_0$ to $D_0D_0D_0$ (homogeneous). Again, although the inferred width of the unexplained error term for each ε_{sys} group varies somewhat depending upon the error model—and hypothesis—adopted, the relative ordering of the aforesaid—Keck LC, VLT, Keck HC (from smallest to largest)—does not. As expected the error widths recovered under the null hypothesis here are generally somewhat greater than those recovered under the (more flexible) dipole hypothesis.

variance in the RLR solution, while Kong et al. (2003) give another structured for improved computational efficiency.

Finally, as stressed in Cameron and Pettitt (2013), it is important to note the power of parallel tempering with RLR for prior-sensitivity analysis. Having explored well beyond the confines of the highest posterior density region at some $\beta(j) < 1$, for which (via RLR) we now have estimated normalization constants, we are well placed to recompute \hat{Z} under a range of alternative prior densities through importance sample reweighting. In this respect we treat the pooled draws from parallel tempering as a (pseudo-)importance sampling proposal density,

$$g(\theta_i) = \sum_{j=1}^m (n[j]/n) [\pi(\theta_i) L(\theta_i)^{\beta(j)}] / \hat{Z}_j. \quad (9)$$

Provided the support of the alternative prior, $\pi_{\text{alt}}(\cdot)$, is contained within that of the default we have the simple unbiased estimator,

$$\hat{Z}_{\text{alt}} = \sum_{i=1}^n \pi_{\text{alt}}(\theta_i) L(\theta_i) / g(\theta_i) / n. \quad (10)$$

Computation of which requires no further likelihood evaluations, only the calculation of $\pi_{\text{alt}}(\theta_i)$ for each $i = 1, \dots, n$.

The uncertainty of this importance sampling estimator will not be much greater than that of our original RLR solution provided the divergence between $\pi_{\text{alt}}(\cdot)$ and $\pi(\cdot)$ is not overwhelming—a condition easily monitored via the effective sample size (Kong et al. 2003). We exploit this valuable property of the RLR estimator to examine the robustness of our BSM results in Section 5 below.

5 MARGINAL LIKELIHOODS

Marginal likelihoods were computed for ten alternative permutations of our four candidate error forms (Section 3.1) over the three ε_{sys} groups of the quasar dataset—in particular, the four general (skeptical) error forms applied homogeneously ($A_0A_0A_0$, $B_0B_0B_0$, $C_0C_0C_0$, $D_0D_0D_0$), plus two non-homogeneous permutations (CAD and CAA) motivated by the observed distributions of residuals ($\Delta\alpha/\alpha - \Delta\alpha/\alpha_{\text{mod}}$) about the King et al. (2012) dipole fit along the equatorial strip of Figure 3—under each of the three competing hypotheses—namely, strict null, monopole-only null, and monopole+ $r(z)$ -dipole. These results, to-

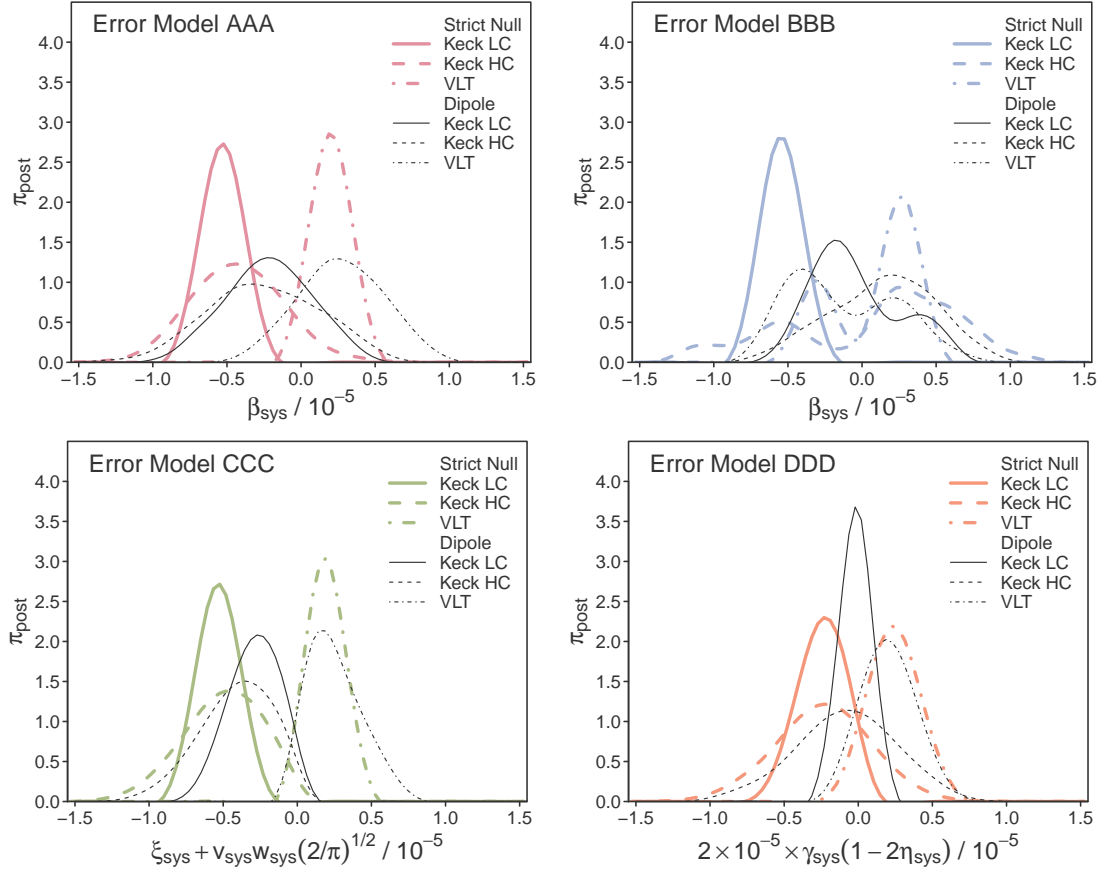


Figure 7. Posterior probability densities for the key parameters (or combinations thereof) governing the error distribution bias (viz. offset of the mode, or in case **D** the mean, from zero) in each of the biased error models: **AAA** to **DDD** (homogeneous). Once again in the interests of illustrative clarity only those posteriors corresponding to our strict null hypothesis and dipole model are compared here. The degree of bias favoured by the results for each ε_{sys} group varies little between error models but greatly between hypotheses—as expected, much larger biases are inferred under the strict null hypothesis than under the dipole hypothesis, owing to the inherent (though of course only partial) degeneracy between the North–South dipole and opposing bias scenarios.

Table 1. Log Marginal Likelihoods for Each Error Model–Hypothesis Pairing Tested Against the Quasar Dataset

	AAA	A₀A₀A₀	BBB	B₀B₀B₀	CCC
Strict Null	-608.0	-616.0	-617.3	-629.2	-608.2
Monopole	-608.5	-615.9	-618.2	-630.5	-608.7
Dipole	-610.5	-610.3	-619.1	-623.1	-608.9
	C₀C₀C₀	DDD	D₀D₀D₀	CAD	CAA
Strict Null	-616.9	-626.3	-627.3	-614.6	-607.7
Monopole	-614.6	-626.5	-629.2	-615.4	-608.0
Dipole	-609.4	-617.8	-617.8	-614.8	-608.2

All quoted $\log \hat{Z}$ have uncertainties $\lesssim 0.1$.

talling thirty separate marginal likelihood estimates, are compiled (in $\log \hat{Z}$ format) in Table 1.

The first point we note here upon consideration of the above is that for the nominal error model (**A₀A₀A₀**) of the Webb et al. team—in which the unexplained source of error in each ε_{sys} group is assumed strictly Normal and strictly unbiased (zero mean and mode)—the log marginal likeli-

hood of the dipole hypothesis ($\log \hat{Z} = -610.3$) exceeds that of both the strict null ($\log \hat{Z} = -616.0$) and monopole-only null ($\log \hat{Z} = -615.9$) alternatives by $\Delta \log \hat{Z} \approx 5.9$. Under the Jeffreys scale for interpretation of Bayes factors (B.F. = $\exp[\Delta \log \hat{Z}]$) such an extreme result (a B.F. > 100) should be considered decisive evidence in favour of the former; broadly consistent at face value (i.e., neglecting for

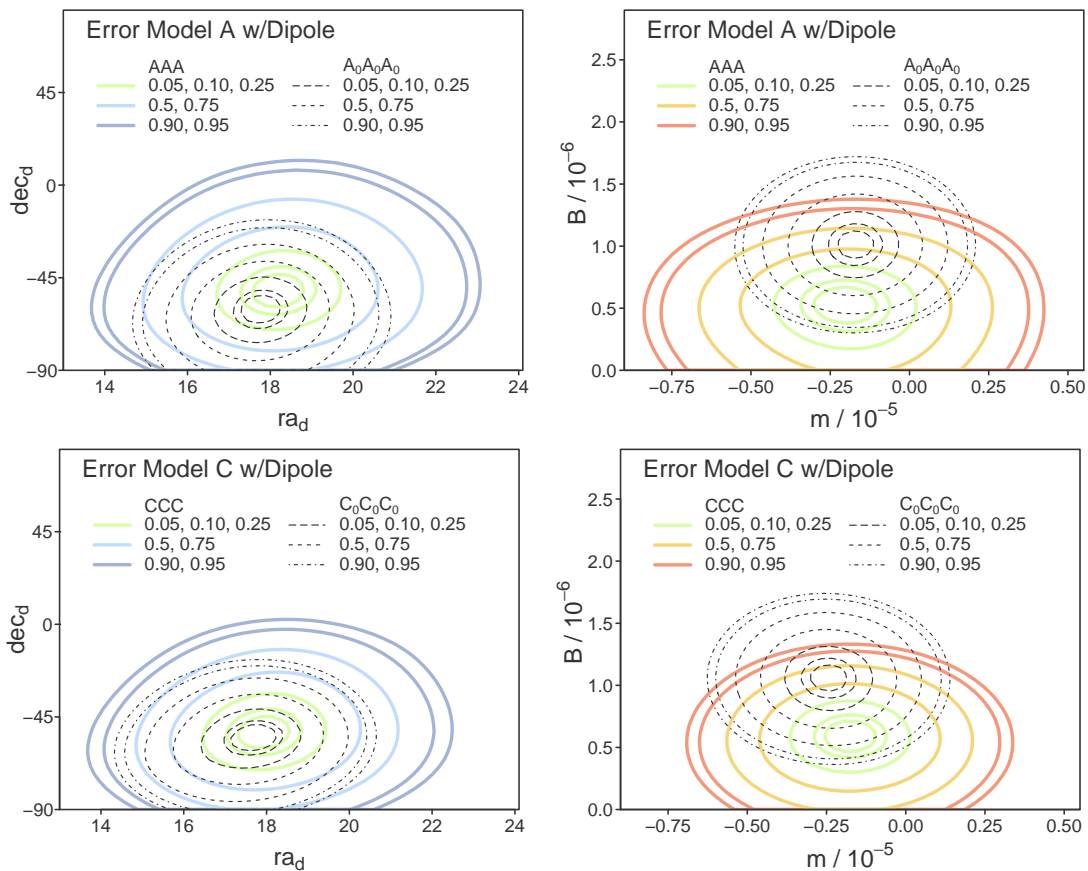


Figure 8. Posterior probability densities for the four key parameters, $\theta_m = \{m, B, ra_d, dec_d\}$, governing the Webb et al. team’s proposed monopole+ $r(z)$ -dipole hypothesis for the apparent spatial variation of $\Delta\alpha/\alpha$ in the fine structure dataset under the following alternative, example forms of the unexplained error term: **AAA** and **A₀A₀A₀** (*top row*); and **CCC** and **C₀C₀C₀** (*bottom row*). We illustrate each posterior via a series of smoothed contours (surrounding the posterior mode and) enclosing increasing fractions of the (marginal) posterior mass from 0.05 to 0.95 in both the m – B plane (giving the strengths of the monopole and dipole components, respectively) and the ra_d – dec_d plane (giving the directions on the celestial sphere). While the posteriors under each error model in the “unbiased” case are both highly concentrated around the maximum likelihood solutions identified by the Webb et al. team under their fitting of the nominal error model (**A₀A₀A₀**)—namely, $\{ra_d \approx 17.5$ hours, $dec_d \approx -60$ degrees $\}$ and $\{m \approx -0.2 \times 10^{-5}$, $B \approx 10^{-6}\}$ —in the biased (skeptical) case the corresponding posteriors are evidently more diffuse and favour markedly a smaller dipole strength.

now both our results for alternative error models and any subjective priors one might hold on the relative merits of these hypotheses) with the Webb et al. team’s bootstrap randomization-based estimate of $\sim 4\sigma$ support for spatial variation in the quasar dataset. (We say “broadly” as, of course, one cannot directly compare p -values against Bayes factors without an explicit calibration of the latter.)

A further inspection of the results compiled in Table 1 reveals that this particular ordering of the null and dipole hypotheses by marginal likelihood recovered under the nominal error model (**A₀A₀A₀**) is in fact conserved across all three alternative error models tested in their “unbiased” cases—namely, **B₀B₀B₀** (heavy tailed), **C₀C₀C₀** (skew), and **D₀D₀D₀** (bimodal). Interestingly, one may also note that the greatest marginal likelihood recovered here for the (*prima facie*) preferred dipole hypothesis under any of these error models is that of $\log \hat{Z} = -609.4$ for the skew Normal form; that is, even with the Ockham’s razor-like tendency of the Bayes factor to favour simpler models (cf. Jeffreys and Berger 1992; Jaynes 2003) we observe here a slight poste-

rior preference for this asymmetric (but zero mode) density relative to its default symmetric alternative.

Turning now to the results in Table 1 for our general (skeptical) error models, which expressly allow for the possibility of opposing systematic biases between the observations from the Keck and VLT telescopes, we discover for all but one permutation tested (**DDD**) a reversal of the above ranking of hypotheses; that is, for error models **AAA**, **BBB**, **CCC**, **CAD**, and **CAA** the strict null and monopole-only null hypotheses are in fact preferred in marginal likelihood over the Webb et al. team’s monopole+ $r(z)$ -dipole hypothesis—although we note that the strength of this preference ranges only between “barely worth mentioning” and “substantial” on the Jeffreys scale. Furthermore, for three of these error models (**AAA**, **CCC**, and **CAA**) the resulting marginal likelihoods for all hypotheses are consistently greater than the maximum recovered for the dipole hypothesis under any unbiased error model; with the greatest maximum likelihood of the present study ($\log \hat{Z} = -607.7$) recovered for **CAA** under the strict null hypothesis. That we recover such support for a skew Normal term in the Keck LC

ε_{sys} group is quite intriguing in that it may offer some insight into the origin of the unexplained errors of this dataset—in particular, it suggests a sole contributor, such as bias in the Keck wavelength calibration solution, rather than the accumulation of many disparate sources converging toward a Normal. Nevertheless, for simplicity, we have elected to focus the ensuing discussion on the almost-as-successful ($\log \hat{Z} = -608.0$) **AAA** model as this was our *a priori* default skeptical proposal and is most similar in form to its (unbiased) nominal rival.

As mentioned earlier, in order to investigate the sensitivity of these results to our choice of priors on both error model and hypothesis parameters we make use here of an important property of the RLR algorithm—namely, that it allows for rapid recomputation of the marginal likelihood (requiring no new likelihood evaluations) under mild modifications to the prior density. In Figure 9 we qualify the subjectivity in this regard of our recovered Bayes factors (B.F.) comparing the strict null against the monopole+ $r(z)$ -dipole hypothesis under the biased error model, **AAA**. In the lefthand panel we examine the impact of varying our hyperparameters, σ_p and σ_q (nominally, $\sigma_p = 0.5 \times 10^{-5}$ and $\sigma_q = 2.0 \times 10^{-5}$), controlling the expected absolute size of the bias, β_{sys} , and the standard deviation, σ_{sys} , respectively, for the unexplained error term. In the righthand panel we apply alternative priors concentrated to varying degrees on the (*a posteriori*) ‘best-fit’ values of the monopole and dipole strength terms, m and B respectively, of the dipole hypothesis. In each case it is evident that large modifications of our stated prior beliefs are required to overturn the weight of evidence against spatial variation in the fine structure constant under this biased error model. Either we must drastically rescale our prior density on the magnitude of the possible error bias to strongly favour biases below the $\sim 10^{-6}$ level, or else provide a convincing post-hoc theoretical justification for the precise strengths of the dipole model’s m and B terms.

6 CONCLUSIONS

Although there exist a number of well-developed cosmological theories within which a time- and/or space-varying fine structure constant can be readily admitted (Bekenstein 1982; Carroll 1998; Marciano 1984; Brax et al. 2003), for many physicists the prior probability of such must be considered small given both our faith in certain long-standing physical principles and the null results of previous experiments designed to test these. In particular, past analyses of the Oklo natural fission reactor (Shlyakhter 1976; Damour and Dyson 1996; Gould et al. 2006), Earth-fallen meteorite samples (Olive et al. 2004), and optical atomic clocks (Fortier et al. 2007; Rosenband et al. 2008) have strongly favoured a scenario of negligible *temporal* variation in α locally; with Rosenband et al. (2008), for instance, determining $|\Delta\alpha/\alpha| < 1.6 \times 10^{-17}$ per year at present on Earth. These results may “daringly” (with respect to the strong assumption of zero higher derivatives) be extrapolated to $|\Delta\alpha/\alpha| < 2 \times 10^{-7}$ since the Big Bang (~ 13.4 Gyr ago); with more prosaic but reliable constraints of $|\Delta\alpha/\alpha| < 0.1$ over this time provided by contemporary analyses of fluctuations in the Cosmic Microwave Background (Rocha et al.

2004; Nakashima, Nagata and Yokoyama 2008; Menegoni et al. 2009; Galli et al. 2010; Calabrese et al. 2011).

Spatial variation in the fine structure constant, on the other hand, has been previously constrained to $|\Delta\alpha/\alpha| < 10^{-4}$ on cosmic scales via both emission and absorption line based quasar studies (Bahcall and Salpeter 1965; Bahcall, Sargent and Schmidt 1967; Ivanchik, Potekhin and Varshalovich 1999). Although the Webb et al. team’s claimed dipole strength contributes an effect well below this level the earlier absorption line results may nevertheless be supposed to have reinforced the prior beliefs of many astronomers (by way of the cosmological principle) that the physical laws of the Universe are spatially invariant. A related expectation that the Universe should appear essentially homogeneous when viewed on sufficiently large scales has also been hitherto well-supported by measurements of the fractal dimension (converging toward three) at large scales in galaxy redshift surveys (Martínez et al. 1998; Scrimgeour et al. 2012) and by the isotropy of the Cosmic Microwave Background (Mandolesi et al. 1986; though see Eriksen et al. 2007 and Clarkson and Barrett 1999). The proposal of a large-scale spatial variation of the fine structure constant across the observable Universe runs into direct conflict with this established paradigm.

To quantify our inherent preference for the strict null hypothesis over the dipole we might therefore, for argument’s sake, suppose a prior log odds ratio of 5, such that $P_{\text{prior}}(\text{strict null})/P_{\text{prior}}(\text{dipole}) \approx 150$. In this conservative scenario, even the Bayes factor of ~ 300 in favour of the dipole under a strictly unbiased, Normal error model is reduced to a posterior odds ratio of just 2 : 1, providing insufficient evidence to convince ourselves beyond doubt that the fine structure constant does indeed vary across the Universe in the manner described. Such a prior hypothesis weighting against the dipole also appears reflected in the relative caution with which both independent cosmologists (Olive, Peloso and Uzan 2011) and the Webb et al. team themselves have at times discussed their results. Moreover, as we have demonstrated herein (cf. Section 5) the skeptical interpretation of null variation under a *biased* error model (in which the current $\Delta\alpha/\alpha$ estimates from the Keck and VLT carry systematic biases of opposing sign) may in fact be preferred from a Bayesian model selection perspective. Thus new observations are undoubtably required if the Webb et al. team or others are to convince a majority of cosmologists to accept the dipole hypothesis.

To this end a dedicated campaign targetting quasars *at the poles of the inferred dipole* has been proposed (Webb et al. 2011; King et al. 2012), and is, in effect, already in progress with a first series of high resolution spectra suitable for $\Delta\alpha/\alpha$ estimation recently obtained on the VLT under Large Program 185.A-0745 (Molaro et al. 2013). Assuming these measurements are subject to both explained and unexplained error terms consistent with those of the original quasar dataset—and supposing further the availability of an equivalent new Keck sample—one can easily forecast the power of such an experimental strategy (and potential alternatives) for settling the null vs. dipole debate. One way to do this is via Monte Carlo simulation of future Bayes factors, assuming the dipole plus (unbiased) Normal error model pairing as truth.

We perform such computational simulations here by

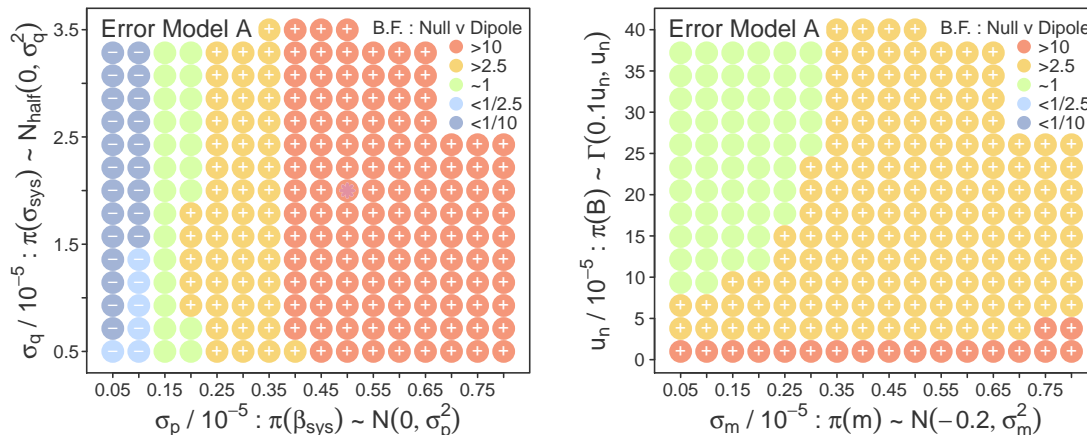


Figure 9. Exploring the prior-sensitivity of the Bayes factor (B.F.) comparing the strict null against the monopole+ $r(z)$ -dipole hypothesis under the skeptical error model, **AAA**. By importance sample re-weighting of our tempered likelihood draws (the normalizations of which were estimated during our earlier RLR run) we can rapidly recompute the log \hat{Z} for each hypothesis, and hence the relative Bayes factor, under alternative priors, $\pi_{\text{alt}}(\cdot)$, with supports enclosed by those of the original. In the lefthand panel we examine the impact of varying our hyperparameters, σ_p and σ_q , controlling the expected absolute size of the bias and the standard deviation (β_{sys} and σ_{sys} , respectively) in the unexplained error term, ε_{sys} . For reference, our original prior corresponds to $\sigma_p = 0.5 \times 10^{-5}$ and $\sigma_q = 2.0 \times 10^{-5}$. In the righthand panel we apply alternative priors concentrated to varying degrees on the (*a posteriori*) ‘best-fit’ values of the monopole and dipole strength terms (m and B , respectively) in the dipole hypothesis. In each case it is evident that large modifications of our stated prior beliefs are required to overturn the weight of evidence against spatial variation in $\Delta\alpha/\alpha$ under this biased error model.

repetition over the following procedure. First, we draw a $\{\theta_m, \theta_e\}$ pair of dipole hypothesis plus $\mathbf{A}_0\mathbf{A}_0\mathbf{A}_0$ error model parameter vectors from the current posterior. For each of n_{new} proposed targets we draw a $\Delta\alpha/\alpha_{\text{obs}}$ estimate accordingly with reference to its nominated telescope (i.e., ε_{sys} group), sightline, and redshift, plus a σ_{obs} sampled (with replacement) from the current quasar dataset. We then compute the marginal log likelihoods of these mock observations under both the strict null and dipole hypotheses, proposing a biased error model for the former and an unbiased error model for the latter, and treating our current posteriors for each as priors. In the case of limited new data this computation can be efficiently and accurately performed via importance sampling from our earlier reverse logistic regression draws; that is, for n_{new} small enough the updated posterior will not differ too markedly from the current posterior. For reference we also perform these simulations with unbiased error models assigned to both hypotheses. The distribution of future Bayes factors under a proposed observing strategy approximated in this manner can be termed the ‘‘predicted posterior odds distribution’’ (or PPOD; Trotta 2007).

In Figure 10 we present the (log) PPOD for three basic targetting strategies, all supposing 25 detected absorbers with $\Delta\alpha/\alpha$ measurements from observations on each of the Keck and VLT telescopes.⁹ In the first, all targets are supposed placed at the current maximum a posteriori sightline of the pole (for the VLT) or anti-pole (for the Keck); in the second, all targets are supposed placed on the dipole’s equator (accessible to both telescopes); and in the third a compromise is made with ten measurements on the equator and the remainder on the pole or anti-pole (as appropriate). As

expected it is indeed the first strategy that gives the greatest chance of recovering the desired additional support of a further +5 on the log Bayes factor of the null vs. dipole comparison with the unbiased error model applied to both. The mixed targetting strategy performs a little worse than the dipole-only case, while the equator-only strategy performs worst of all. With regards to choosing between the null and dipole when allowing for a biased error model on the former the performance of our three strategies is in fact reversed, such that the equatorial design offers the greatest chance of a conclusive outcome. An intuitive interpretation of this result is simply that for distinguishing between a biased and unbiased error model under two competing hypotheses the most effective design is to observe at locations where those underlying hypotheses are already in close agreement.

Finally it is worth noting the wide range of predicted Bayes factors under all these possible observing strategies, which are so broad as to include a non-trivial possibility of rejecting the true hypothesis despite an optimal experimental design. This phenomenon arises principally from the broad range allowed for the strength parameter of the dipole, B , under the current posterior (see Figure 8), which gives non-negligible weight to the possibility that the dipole signal is far too small (with respect to the observational errors) to confidently recover from an $n_{\text{new}} = 50$ sample.

Thus, we reach the final conclusions of our Bayesian re-analysis of the quasar dataset. Namely, that: (I) given both our incomplete understanding of the observational errors and our limited theoretical (prior) expectations regarding the properties of any spatial variation in the fine structure constant, the present observational coverage (featuring limited overlap of the two telescopes for which opposing biases might be suspected) must be deemed inadequate to properly distinguish the Webb et al. team’s proposed dipole field from the (strict or monopole) null; and (II) one cannot afford to overlook the importance of observations along the equator

⁹ The choice of 25 new absorbers from each telescope (i.e., $n_{\text{new}} = 50$) is consistent with expectations for the ongoing VLT Large Program (Molaro et al. 2013).

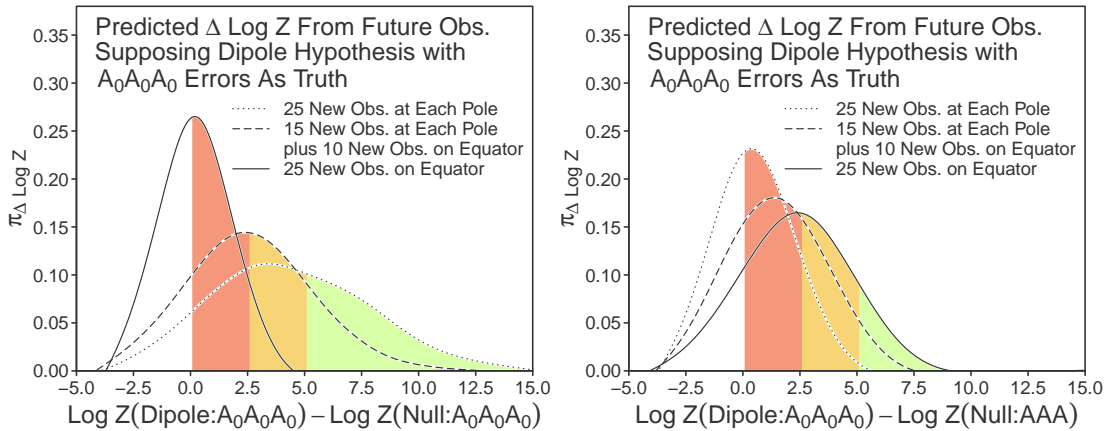


Figure 10. The predicted power of future quasar observations for increasing the log Bayes factor in favour of the dipole hypothesis (supposed here as truth) under the nominal (unbiased, Normal) error model in the lefthand panel and under our default skeptical (biased, Normal) error model in the righthand panel. In each case we suppose the availability of 25 new $\Delta\alpha/\alpha$ estimates from each of the VLT and Keck telescopes subject to both explained and unexplained error terms consistent with those of the original quasar dataset. Three alternative targetting strategies have been simulated: (i) all targets placed at the current maximum a posteriori sightline of the pole (for the VLT) or anti-pole (for the Keck); (ii) all targets placed on the dipole’s equator; and (iii) a compromise with ten measurements on the equator and the remainder on the pole or anti-pole (as appropriate). Note that the future log posterior odds ratio for each case should be considered the sum of the future log Bayes factor considered above with the current log Bayes factor from the original quasar dataset (lefthand panel: +5.7; righthand panel: -2.5) minus our log prior odds ratio of 5 against the dipole.

of the alleged dipole in addition to those proposed along its poles when planning future campaigns with the Keck and VLT telescopes for the purpose of settling this debate.

We have also demonstrated in this study the utility of the reverse logistic regression technique for marginal likelihood computation with efficient prior-sensitivity analysis.

ACKNOWLEDGMENTS

[1] E.C. is grateful for financial support from the Australian Research Council.

REFERENCES

- Albrecht A. and Magueijo J., 1999, *Phys. Rev. D*, 59, 043516
- Andrae R., Shulze-Hartung T. and Melchior P., 2010, preprint(arXiv:1012.3754)
- Bahcall J.N. and Salpeter E.E., 1965, *ApJ*, 142, 1677
- Bahcall J.N., Sargent W.L.W. and Schmidt M., 1967, *ApJ*, 149, L11
- Barrow J.D., 1999, *Phys. Rev. D*, 59, 043515
- Barrow J.D. and Magueijo J., 2000, *ApJ*, 532, L87
- Bekenstein J.D., 1982, *Phys. Rev. D*, 25, 1527
- Berengut J.C, Kava E.M. and Flambaum V.V., 2012, *A&A*, 542, A118
- Berger J.O. and Pericchi L.R., 1996, *JASA*, 91, 109
- Borie E., 1986, *Metrologia*, 22, 140
- Bosch J.F., 2011, Thesis: Modeling techniques for measuring galaxy properties in multi-epoch surveys, preprint(arXiv:1109.1033)
- Bouchendira R., Cladé P., Guellati-Khélifa S., Nez F. and Biraben F., 2011, *Phys. Rev. Lett.*, 106, 080801
- Brax Ph., van de Bruck C., Davis A.-C. and Rhodes C.S., 2012, *Astrophys. Space Sci.*, 283, 627
- Burbidge E.M, Lynds C.R. and Burbidge G.R., 1966, *ApJ*, 144, 447
- Calabrese E., Menegoni E., Martins C.J.A.P., Melchiorri A. and Rocha G., 2011, *Phys. Rev. D*, 84, 023518
- Cameron E. and Pettitt A.N., 2013, preprint(arXiv:1301.6450)
- Carlip S. and Vaidya S., 2003, *Nature*, 421, 498
- Carroll S.M., 1998, *Phys. Rev. Lett.*, 81, 3067
- Chipman H., George E.I. and McCulloch R.E., 2001, *Lecture Notes–Monograph Series*, 65
- Clarkson C.A. and Barrett R.K., 1999, *Class. Quant. Grav.*, 16, 3781
- Damour T. and Dyson F., 1996, *Nuclear Phys. B*, 480, 37
- Davies P.C.W., Davis T.M. and Lineweaver C.H., 2002, *Nature*, 418, 602
- Dzuba V.A., Flambaum V.V. and Webb J.K., 1999, *Phys. Rev. A*, 59, 230
- Eriksen H.K, Banday A.J, Górski K.M., Hansen F.K. and Lilje P.B., 2007, *ApJL*, 660, 81
- Feroz F., Hobson M.P., Cameron E. and Pettitt A.N., 2013, preprint(arXiv:1306.2144)
- Fortier T.M, Ashby N., Bergquist J.C., Delaney M.J., Didams S.A., Heavner T.P., Hollberg L., Itano W.M., Jefferts S.R., Kim K., Levi F., Lorini L., Oskay W.H., Parker T.E., Shirley J. and Stalkner J.E., 2007, *Phys. Rev. Lett.*, 98, 070801
- Galli S., Matteo M., Melchiorri A., Pagano L., Sherwin B.D. and Spergel D.N., 2010, *Phys. Rev. D*, 82, 123504
- Gelman A., Carlin J.B., Stern H.S. and Rubin D.B., 2003, *Bayesian Data Analysis*, 3rd Edition, Chapman & Hall/CRC, Boca Raton, USA
- Geyer C.J., 1992, *Statist. Sci.*, 7, 473
- Geyer C.J., 1994, *Technical Report 568*
- Gould C.R., Sharapov E.I. and Lamoreaux S.K., 2006, *Phys. Rev. C*, 74, 024607
- Griest K., Whitmore J.B., Wolfe A.M., Prochaska J.X.,

- Howk J.C. and Marcy G.W., 2010, *ApJ*, 708, 158
- Griffiths D.J., 2005, *Introduction to Quantum Mechanics*, 2nd ed., Pearson Prentice Hall, Upper Saddle River, NJ
- Hanneke D., Fogwell S. and Gabrielse G., 2008, *Phys. Rev. Lett.*, 100, 120801
- Hogg D.W., 1999, preprint(arXiv:9905116)
- Ivanchik A.V., Potekhin A.Y. and Varshalovich D.A., 1999, *A&A*, 343, 439
- Jaynes E.T., 2003, *Probability theory: The logic of science*, Cambridge University Press, Cambridge, UK
- Jeffreys H., 1961, *Theory of probability*, 3rd ed, Clarendon Press, Oxford, UK
- Jeffreys W.H. and Berger J.O., 1992, *Amer. Sci.*, 80, 64
- Kadane J.B. and Lazar N.A., 2004, *JASA*, 99, 279
- Kass R.E. and Raftery A.E., 1995, *JASA*, 90, 773
- Kendall D., 1938, *Zeit. Astro.*, 16, 308
- King J.A., Mortlock D., Webb J. and Murphy M., 2010, *High. Astro.*, 15, 318
- King J.A., Webb J.K., Murphy M.T., Flambaum V.V., Carswell R.F., Bainbridge M.B., Wilczynska M.R., and Koch F.E., 2012, *MNRAS*, 422, 3370
- Kong A., McCullagh P., Meng X.L., Nicolae D. and Tan Z., 2003, *JRSS B.*, 65, 585
- Lamoreaux S.K. and Torgerson J.R., 2004, *Phys. Rev. D*, 69, 121701
- Levshakov S.A, Combes F., Boone F., Agafonova I.I., Reimers D. and Kozlov M.G., 2012, *A&A*, 540, L9
- Mallows C.L., 1995, *Technometrics*, 37, 362
- Mandolesi N., Calzolari P., Cortiglioni S., Delpino F., Sironi G., Inzani P., Deamicis G. et al., 1986, *Nature*, 319, 751
- Marciano W., 1984, *Phys. Rev. Lett.*, 52, 489
- Martínez V.J., Pons-Bordería M.-J., Moyeed R.A. and Graham M.J., 1998, *MNRAS*, 298, 1212
- Menegoni E., Galli S., Barlett J.G., Martins C.J.A.P. and Melchiorri A., 2009, *Phys. Rev. D*, 80,087302
- Moffat J.W., 1993, *Int. J. Mod. Phys. D*, 2, 351
- Molaro P., Levshakov S.A., Monai S., Centurión M., Bonifacio P., D'Odorico S. and Monaco L., 2008, *A&A*, 481, 559
- Molaro P. et al., 2013, *A&A*, 555, A68
- Murphy M.T., Webb J.K., Flambaum V.V., Prochaska J.X. and Wolfe A.M., 2001, *MNRAS*, 327, 1237
- Murphy M.T., Webb J.K. and Flambaum V.V., 2003, *MNRAS*, 345, 609
- Nakashima M., Nagata R. and Yokoyama J., 2008, *Progr. Theor. Phys.*, 120, 1207
- Nason G.P., 2006, *Stat. Prob. Lett.*, 76, 1280
- Olive K.A, Pospelov M., Qian Y.-Z., Manhès G., Vangioni-Flam E., Coc A. and Cassé M., 2004, *Phys. Rev. D*, 69, 027701
- Olive K.A, Peloso M. and Uzan J.-P., 2011, *Phys. Rev. D*, 83, 43509
- Pewsey A., 2000, *Comm. Stat.*, 29, 2459
- Rocha G., Trotta R., Martins C.J.A.P., Melchiorri A., Avelino P.P., Bean R. and Viana P.T.P., 2004, *MNRAS*, 352, 20
- Rosenband T., Hume D.B., Schmidt P.O., Chou C.W., Brusch A., Lorini L., Oskay W.H., Brullinger R.E., Fortier T.M., Stalnaker J.E., Diddams S.A., Swann W.C., Newbury N.R., Itano W.M., Wineland D.J. and Bergquist J.C., 2008, *Science*, 319, 1808
- Rousseuw P.J., 1984, *JASA*, 74, 871
- Savedoff J.D., 1956, *Nature*, 178, 688
- Scrimgeour M., Davis T., Blake C., James J.B., Poole G., Staveley-Smith L., Brough S., Colless M. et al., 2012, *MNRAS*, 425, 116
- Shlyakhter A.I., 1976, *Nature*, 264, 340
- Stockton A.N. and Lynds C.R., 1966, *ApJ*, 144, 451
- Swendsen R.H. and Wang J.S., 1986, *Phys. Rev. Lett.*, 57, 2607
- Trotta R., 2007, *MNRAS*, 378, 72
- Webb J.K., Flambaum V.V., Churchill C.W., Drinkwater M.J. and Barrow J.D., 1999, *Phys. Rev. Lett.*, 82, 884
- Webb J.K., Murphy M.T., Flambaum V.V., Dzuba V.A., Barrow J.D., Churchill C.W., Prochaska J.X. and Wolfe A.M., 2001, *Phys. Rev. Lett.*, 87, 091301
- Webb J.K., King J.A., Murphy M.T., Flambaum V.V., Carswell R.F. and Bainbridge M.B., 2011, *Phys. Rev. Lett.*, 107, 191101
- Weinberg M., 2012, *Bayesian Anal.*, 7, 737
- Weiss A., Walter F., Downes D., Carilli C.L., Henkel C., Menten K.M. and Cox P., 2012, *ApJ*, 753, 102
- Whitmore J.B., Griest K. and Murphy M.T., 2010, *ApJ*, 723, 89
- Wilcoxon F., 1945, *Biometrics Bull.*, 1, 80
- van Dyk D.A., Degennaro S., Stein N., Jefferys W.H and von Hippel T., 2009, *An. App. Stat.*, 3, 117